GRI-81/0111

Physical Engineering and Environmental Aspects of Ocean Kelp Farming

Final Report: January 1982 – September 1982

Gas Research Institute
8600 West Bryn Mawr Avenue
Chicago, Illinois 60631

PHYSICAL ENGINEERING AND ENVIRONMENTAL ASPECTS OF OCEAN KELP FARMING

FINAL REPORT

(January 1982 - September 1982)

Prepared by

D. P. Wang and J. D. Ditmars

Energy and Environmental Systems Division
Argonne National Laboratory
Argonne, Illinois 60439

Argonne Report Number ANL/EES-TM-208

For

GAS RESEARCH INSTITUTE

Contract No. 5081-351-0515

GRI Project Managers

K. T. Bird
Supply Division

C. A. Cahill
Environment, Safety and Distribution Division

October 1982

GRI DISCLAIMER

LEGAL NOTICE This report was prepared by Argonne National Laboratory as an account of work sponsored by the Gas Research Institute (GRI). Neither GRI, members of GRI, nor any person acting on behalf of either:

a. Makes any warranty or representation, express or implied, with respect to the accuracy, completeness, or usefulness of the information contained in this report, or that the use of any apparatus, method, or process disclosed in this report may not infringe privately owned rights; or

b. Assumes any liability with respect to the use of, or for damages resulting from the use of, any information, apparatus, method, or process disclosed in this report.

REPORT DOCUMENTATION PAGE	1. REPORT NO. GRI-81/0111, ANL/EES-TM-208	2.	3. Recipient's Accession No.
4. Title and Subtitle Physical Engineering and Environmental Aspects of Ocean Kelp Farming			5. Report Date October, 1982 6.
7. Author(s) D. P. Wang and J. D. Ditmars			8. Performing Organization Rept. No.
9. Performing Organization Name and Address Energy and Environmental Systems Division Argonne National Laboratory Argonne, Illinois 60439			10. Project/Task/Work Unit No. 11. Contract(C) or Grant(G) No. (C) 5081-351-0515 (G)
12. Sponsoring Organization Name and Address Gas Research Institute 8600 West Bryn Mawr Avenue Chicago, Illinois 60631			13. Type of Report & Period Covered Final 14.

15. Supplementary Notes

16. Abstract (Limit: 200 words)

The physical aspects of ocean kelp farming were studied in the context of farms sited in nearshore coastal waters. Analyses and models were employed to investigate the physical oceanographic and ocean engineering problems underlying conceptual designs of nearshore kelp farms. The areas addressed include interactions between ocean coastal currents and kelp farms, distribution and transport of fertilizer in and around the farm, interactions between surface water waves and kelp farms, effects on adjacent shorelines of wave field modifications due to the farm, and wave forces on kelp plants.

For the range of coastal conditions and farm configurations examined, it was found that the flow of ocean currents is significantly retarded within the farm and flows are deflected in a narrow band around the farm; substantial losses from the farm of applied fertilizer result from advection within the farm; water wave heights can be significantly reduced within the farm due to the kelp, and a shadow zone of reduced waves may extend significantly shoreward of the farm; the shadow zone may, under certain conditions, result in shoreline modification; and wave forces on the kelp have inertial components of the same order of magnitude as buoyancy forces.

17. Document Analysis a. Descriptors

b. Identifiers/Open-Ended Terms

c. COSATI Field/Group

18. Availability Statement	19. Security Class (This Report)	21. No. of Pages
	20. Security Class (This Page)	22. Price

Title	Physical Engineering and Environmental Aspects of Ocean Kelp Farming
Contractor	Energy and Environmental Systems Division Argonne National Laboratory
	GRI Contract Number 5081-351-0515
Principal Investigators	J. D. Ditmars and D. P. Wang
Report Period	January - September 1982 Final Report
Objective	To provide technical support to the GRI marine biomass program with emphasis on interactions of an ocean kelp farm with currents and waves, nutrient distributions in the farm, and impacts of the kelp farm on the physical ocean environment.
Technical Perspective	Development of nearshore ocean kelp farms to provide the feedstock for the production of substitute natural gas (methane) and by-products requires an understanding of the physical interactions of the farm with the ocean. Knowledge of these interactions is as important to the study of ocean kelp farms as is knowledge of kelp growth and digester processes for methane production. Present knowledge of kelp-farm/ocean interactions is limited, and analyses that are generally applicable to nearshore ocean kelp farm environments are needed.
Results	Analyses were conducted and numerical models were developed to study the interactions of ocean currents and waves with a nearshore kelp farm. These models were applied to simple farm configurations in generic coastal environments to provide preliminary estimates of the magnitude of the interactions. The coastal-current/farm interaction model indicated that, inside the farm, flow is reduced to 30-40% of the incoming ambient current. This circulation model provided the basis for a primitive fertilizer balance model that showed substantial losses of applied fertilizer due to current flow within the farm. A model of wave height reduction within the kelp farm demonstrated the dependence of wave height on the hydrodynamic and geometric characteristics of the waves and the kelp. Modifications of the wave field behind a nearshore farm were modeled, and preliminary results suggested that, under certain conditions, the shoreline may be modified due to changes in the wave field. An examination of the forces on kelp under conditions of combined waves and currents indicated

that inertial forces should be included in wave force calculations.

Technical Approach

The general aspects of a conceptual design for a nearshore kelp farm in preparation for GRI by another contractor were reviewed, as was previously sponsored offshore ocean kelp farm research. The primary problems related to physical interactions between the ocean and a nearshore kelp farm were identified, and preliminary analyses of those problems were undertaken to generate quantitative estimates of the significance of each issue. Existing numerical models and analyses were adapted for use in this project.

Project Implications

This research project has clarified important physical oceanographic and environmental issues associated with the nearshore kelp farms being studied in the GRI marine biomass program. The gas supply-oriented conclusions and recommendations will provide the input needed eventually to implement a nearshore kelp farm design that will withstand physical oceanographic processes and to design an efficient fertilization scheme. These conclusions also provide important insights into the design of a farm geometry that would increase cost effectiveness and minimize experimental hardware research costs. The conclusions and recommendations will also guide environmental planning for this advanced biomass technology in the examination of shoreline changes resulting from nearshore farms and in the collection of field data to verify the modified model for predicting nutrient distribution.

GRI Project Managers:

K. T. Bird, Project Manager
Substitute Natural Gas Research

C. A. Cahill, Project Manager
Biomass Environmental Research

CONTENTS

FIGURES

1 INTRODUCTION

The marine biomass program at the Gas Research Institute (GRI) began in 1974. The general purpose of the program has been to develop a commercial-scale system for producing methane gas from marine biomass. Research undertaken in support of this program has addressed the growth and cultivation of macroalgae, the anaerobic digestion of the algae, and marine farming concepts (including the deployment of a small "at sea" test farm). A general summary of early program activities is provided by Leone (1980). The macroalgae under consideration has been the giant brown kelp, *Macrocystis pyrifera*.

In 1981, the basic concepts of commercial open-ocean kelp farming were being developed by the General Electric Company (GE) for GRI. Planning included the development of a set of basic parameters for a hypothetical 1000-mi^2 commercial-size farm suited for the offshore waters of southern California. This hypothetical kelp farm was described at a 1981 workshop on the environmental impact of marine biomass production (Ritschard et al., 1981). Several issues related to the physical interactions of an open-ocean kelp farm with the ocean were prominent among the conclusions and recommendations of the workshop. The supply and distribution of nutrients for the farm, downstream environmental effects of nutrient transport, and ocean engineering questions were identified as areas in which additional knowledge was required for adequate assessments of the operational success and environmental impact of open-ocean kelp farming.

This project was initiated in 1982 in support of an evaluation of a conceptual design for nearshore ocean kelp farming. The General Electric Company was to explore the conceptual design of a hypothetical kelp farm in the nearshore coastal waters of southern California (General Electric Company, 1982). Many of the issues of kelp farm interactions with the ocean important for open-ocean farms are also important for nearshore farms; issues associated with impacts on the coastal environment are more significant for the nearshore farm concept. Since few studies have been made of the physical aspects of ocean kelp farming, the present project was initiated to provide GRI both with information useful for the assessment of the conceptual design and with an initial technical framework for the more general understanding of the physical aspects of marine biomass activities. Limited available information on the physical oceanographic and ocean engineering aspects of nearshore marine biomass farming makes a general investigation of this topic particularly appropriate.

This project has provided technical support to the Substitute Natural Gas Research Department and the Environment and Safety Research Department of GRI with regard to the physical aspects of ocean kelp farming. Argonne National Laboratory (ANL) has investigated some of the key areas in which knowledge is required for the conceptual design of nearshore kelp farms. The topics considered include:

Interactions between ocean currents and kelp farms,

Fertilizer distribution systems,

Interactions between ocean waves and kelp farms,

Modifications to the nearshore environment,

Environmental loading on kelp farms and restraint systems, and

Downstream environmental effects.

The approach taken to study problems in the above areas involved three steps:

Examine the problem and identify the features of the problem essential for nearshore kelp farm conceptual design,

Provide preliminary solutions to each problem in terms of the general characteristics of the Southern California coastal region and the general features of the initial GE concept of 3000- to 5000-acre farms in water depths up to 60 feet, and

Determine the implications of the two previous steps for generic problems of nearshore kelp farming.

The problems are, in most cases, complex and have received little attention in previous investigations of marine biomass systems. Thus, definitive and comprehensive results were not the goal of these preliminary investigations. Rather, a basis was sought for determining critical issues that require additional study as part of the GRI marine biomass program.

In this project, ANL was assisted by a subcontractor, Coastal and Offshore Engineering and Research, Inc. (COER). ANL assigned to COER the tasks of investigating the problems that were primarily related to ocean engineering analyses. ANL's efforts concentrated on the circulation patterns in and around the farm, implications of such modifications for fertilizer distribution schemes, and downstream environmental impacts.

The investigations by COER were documented in a final report entitled "Ocean Engineering Aspects of Coastal Kelp Farming," which is appended to this report. The results of the COER studies are summarized in the body of this report, with references to the Appendix for details. Several of the analyses performed by Argonne and COER involve the use of numerical models.

Each of the major problem areas considered in this project is discussed in the subsequent sections of this report.

2 INTERACTIONS BETWEEN OCEAN CURRENTS AND KELP FARMS

An understanding of the interactions of the ambient ocean current with a nearshore kelp farm is important to the development of kelp farming systems for at least three reasons: (1) the distribution of the fertilizer added to the farm is controlled in large measure by the circulation patterns within the farm, (2) the modification of the current field by the farm affects the restraint and substrate system designs, and (3) downstream environmental impacts are controlled, in part, by circulation patterns in and around the kelp farm.

Measuring kelp farm modifications to coastal currents is, of course, not possible because no such farms exist. Measurements of currents within small naturally occurring kelp beds would be helpful, but existing data on currents within kelp beds appear to be limited to less than two weeks of measurements at one location (G.A. Jackson, Scripps Institution of Oceanography, La Jolla, Calif., personal communication, 1982). Thus, a model of coastal currents modified to account for the presence of a kelp farm (in terms of its effect on circulation) was employed for the initial investigation of the interactions between ambient coastal currents and a nearshore kelp farm.

The numerical model is a two-dimensional, depth-integrated model of circulation. For simplicity, it is assumed that the water depths in the regions modeled are constant (the model can handle variable depths, however), the waters are not density-stratified (a constraint imposed by the model used), and the kelp plants are uniformly distributed within the farm. The effect of the presence of the kelp farm is simulated in the model by modifying the resistance to motion within the region of the coastal environment occupied by the farm.

Currents passing through a kelp farm will be deflected and dissipated due to the drag forces exerted on plants. Assuming a vertically uniform current, the form drag force, F_D, on an individual plant is:

$$F_D = \tfrac{1}{2} \rho C_D D h u^2 \qquad (1)$$

where:

ρ = water density,

C_D = drag coefficient,

D = effective plant diameter,

h = water depth, and

u = current velocity.

When currents are strong, the entire plant may be submerged and the additional frictional (skin) drag may increase the effective drag coefficient. The form drag force per unit volume of water within the farm is:

$$f_D = \frac{F_D}{h} = \rho \frac{\beta}{h} u^2 \tag{2}$$

where:

$$\beta = \tfrac{1}{2} C_D \frac{Dh}{b^2} \text{ within the kelp farm, and} \tag{3}$$

b = plant spacing.

Equation 3 indicates that the drag force depends on the drag coefficient, plant density, and current velocity.

The depth-integrated equations of motion and continuity in water of constant density for a nondivergent flow are:

$$\frac{\partial}{\partial t} u + \frac{\partial}{\partial x} (uu) + \frac{\partial}{\partial y} (uv) = - \frac{1}{\rho} \frac{\partial}{\partial x} P - \frac{\beta}{h} uU \tag{4}$$

$$\frac{\partial}{\partial t} v + \frac{\partial}{\partial x} (uv) + \frac{\partial}{\partial y} (vv) = - \frac{1}{\rho} \frac{\partial}{\partial y} P - \frac{\beta}{h} vU \tag{5}$$

$$\frac{\partial}{\partial x} u + \frac{\partial}{\partial y} v = 0 \tag{6}$$

where:

u = alongshore velocity component,

v = offshore velocity component,

P = pressure,

$U = (u^2 + v^2)^{1/2}$, and

β = Eq. 3 inside the kelp farm
0.01 in the open ocean.

The equations of motion and continuity have been averaged over turbulent time scales, as well as depth. Resistance or frictional forces are included in a single term by means of a frictional coefficient β. The frictional coefficient β is evaluated from Eq. 3 within the kelp farm, and its open-ocean value is based on direct measurements in coastal waters.

Equations 4-6 can be reduced to a vorticity equation upon cross-differentiation:

$$\frac{\partial}{\partial t} \nabla^2 \psi = - \frac{U}{H} \left\{ \beta \left[\left(1 + \frac{\psi_x^2}{U^2} \right) \psi_{xx} + \left(1 + \frac{\psi_y^2}{U^2} \right) \psi_{yy} \right] + \beta_x \psi_x + \beta_y \psi_y \right\} \tag{7}$$

where:

ψ is the streamfunction defined by $u = -\psi_y$ and $v = \psi_x$, (8)

∇^2 is a divergence operator,

$U = (\psi_x^2 + \psi_y^2)^{1/2}$ is the current speed, and

β_x and β_y are the gradients in β between the inside and outside of the farm.

In Eq. 7, the nonlinear advection term is small compared to the friction term for typical coastal currents (on the order of 0.1 m/s) and is neglected. The inflow condition is specified at $x \to -\infty$ (far upstream), and a radiation condition is used at outflow boundaries. At the coast ($y = 0$), the flow normal to the boundary is set to zero. Numerical solution of Eq. 7 is based on a relaxation method. The computational region is shown in Fig. 1.

The specific values of parameters related to the resistance to flow within the farm are not known, but can be estimated on the basis of other flow situations. Likewise, the specific site characteristics of a potential kelp farm and the configuration of the farm itself are not known. However, for our purposes in this investigation, values estimated to be appropriate were used to determine the magnitude of current-farm interactions indicated by the model. Values of some parameters were varied to determine the sensitivity of the model results. For the basic computations made with the circulation model for a nearshore kelp farm, the following values were assumed:

$D = 0.3$ m (1 ft),

$b = 1.5$ m (5 ft),

$h = 15$ m (50 ft), and

$C_D = 1.0$.

The resulting value for β within the farm is 1. For all the computations, an undisturbed ambient current flows parallel to the coast toward a rectangular farm oriented with its long axis parallel to the coast. The velocity field or streamline pattern throughout the computational region (inside and outside the farm) was determined for several different situations.

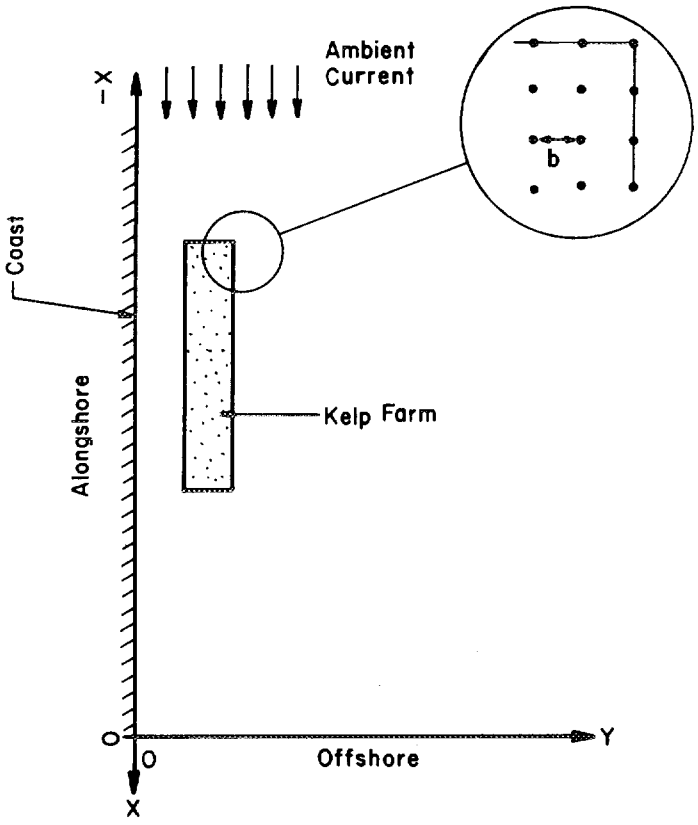

Fig. 1 Schematic Diagram of Plan View of Nearshore Kelp Farm

For a uniform inflow of ambient current, steady-state flow fields were obtained for a 10 km × 1 km farm centered 1 km offshore. Figure 2a shows the streamfunction distribution; the flow pattern can also be inferred by noting that the current follows the direction of streamline and the speed is proportional to the normal gradient of the streamline (several representative velocity vectors are superimposed on the streamfunction for clarity). Most of the inflow is deflected at the front edge of the kelp farm, due to the large increase in friction. The results of the computations indicate that the flow is uniform in the kelp farm, moving downstream at about 35% of the incoming velocity. Around the kelp farm, the alongshore velocity is increased by 42% at the shoreward side and 32% at the seaward side. The cross-shore velocity, which is zero far from the kelp farm, reaches a maximum of 25% of the incoming speed at the front and back sides of the kelp farm.

Figure 2b shows the steady-state streamfunction distribution for a 20 km × 1 km farm. In the larger farm, the interior velocity is about 34% of the incoming speed. So, the flow pattern remains essentially the same for a kelp farm whose length is much greater than its width. When the length becomes comparable with the width, the deflection of the incoming flow is weaker. For example, computations of flow in a 2 km × 1 km kelp farm indicate that the interior velocity if 40% of the incoming speed.

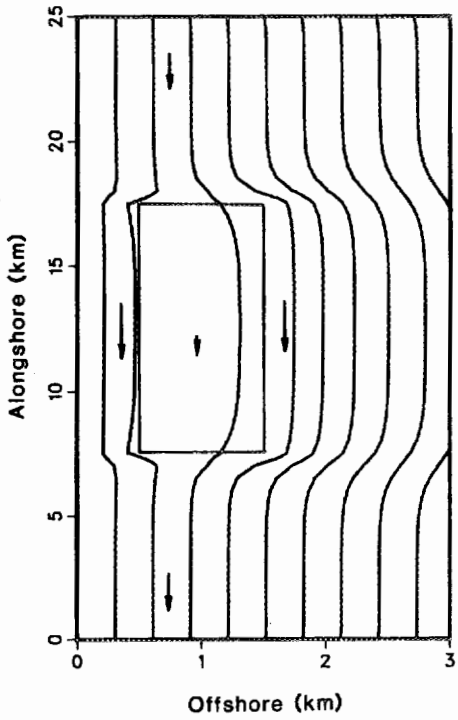

a. 10 km × 1 km Farm (β = 1)

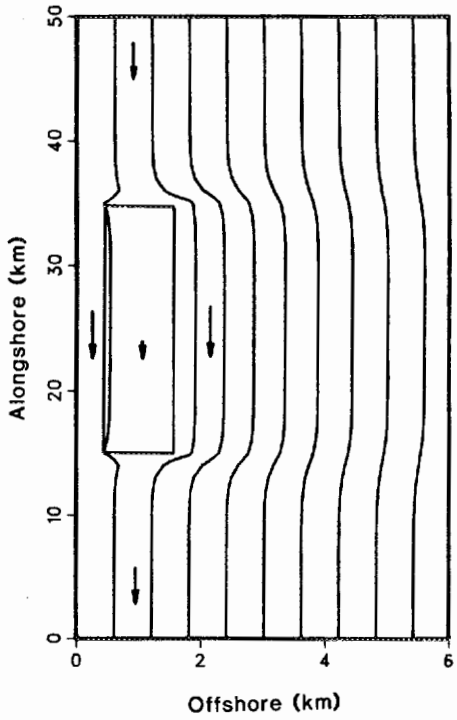

b. 20 km × 1 km Farm (β = 1)

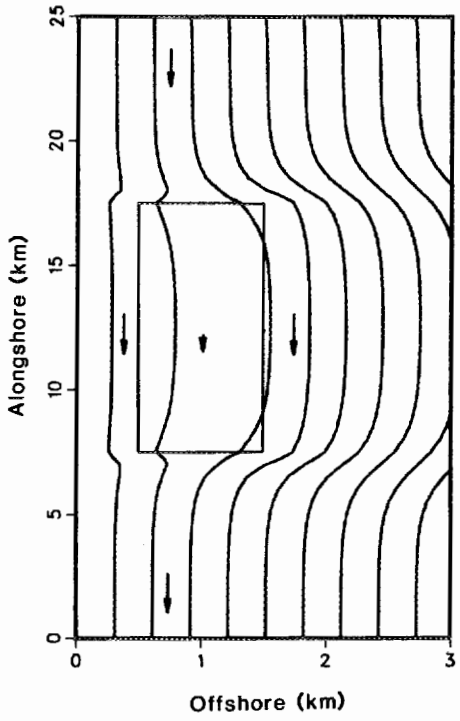

c. 10 km × 1 km Bed (β = 0.1)

Fig. 2 Streamfunction Distributions for Kelp Farms and Natural Kelp Bed (showing farm or bed boundary and representative velocity vectors)

Figure 2c shows the streamfunction distribution for a 10 km × 1 km natural kelp bed, with $\beta = 0.1$ inside the kelp bed. A smaller interior frictional coefficient corresponds to a plant density that is lower than would be found in a kelp farm and that is on the order of that in a natural kelp bed. The velocity inside the kelp bed is about 39% of the incoming velocity -- slightly larger than in the 10 km × 1 km farm case (Fig. 2a). On the other hand, the alongshore velocity only increases by about 10% around the kelp bed. Compared to the farm case (Fig. 2a), the streamlines tend to bend more offshore, i.e., a natural kelp bed will deflect the incoming flow more toward the offshore direction. In the case of a bed or farm distant from the shore, the bed with its lower frictional resistance would deflect the flow less than a farm would. The interaction of the shoreline and bed- or farm-induced flow is thought to produce the result seen here.

In summary, our analysis indicates significant flow modification by a kelp farm. Inside a kelp farm, the flow is retarded to 30-40% of the incoming current. The deflected current moves around the kelp farm in a narrow band about 1 km wide.

While all possible scenarios of coastal environment and kelp farm configuration were not examined in this analysis, the model employed can be used for additional cases. The noteworthy advantages of this technique over a one-dimensional current penetration analysis are that (1) the two-dimensional flow pattern is closer to reality than is the one-dimensional assumption that flow goes directly into the farm and stops, (2) the existence of relatively large current shear near the farm edges may be important for design purposes, and (3) the interior currents are small, but not zero, and do transport material through the farm.

3 NUTRIENT DISTRIBUTION AND TRANSPORT

The distribution of nutrients throughout the kelp farm is important regardless of whether the source of the nutrients is deep, nutrient-rich ocean water or externally supplied fertilizer. The initial distribution of nutrients throughout the farm and the subsequent transport of the nutrients by the water in the farm are important and related problems that directly affect farm design and operation and downstream environmental impact. The efficient uptake of applied nutrients by the kelp is important not only in terms of plant yield but also in terms of distribution system costs, fertilizer costs, and potential downstream environmental costs.

The issues of efficient fertilizer distribution and impact assessment are complex, and we have not attempted to undertake a comprehensive study of them. We have, however, constructed a relatively simple numerical model of nutrient conservation to illustrate the type of rational analysis that can be applied to this problem in general and to demonstrate the profound effects of physical transport on fertilizer distribution in particular.

The approach employed was to write the conservation of mass equation for a chemical species (nitrogen, for example) and to use the circulation model described in Section 2 to determine the advection (transport) of the species in and around the farm in response to a prescribed dose of fertilizer. Since depth-averaged circulation was employed, vertical concentration profiles were not considered. Thus, in the model, the kelp does not deplete nutrients selectively over the water column. Losses of nutrients due to bottom and horizontal diffusion effects are neglected in this formulation. The initial spatial distribution of fertilizer over the farm can easily be varied within the model, but for the purposes of this example the fertilizer distribution systems are kept simple. (Ultimately, of course, one would want to feed the information on the distribution of nutrients within the farm back into new designs for fertilizer distribution schemes.)

The depth-integrated equation of conservation of mass for a chemical species (nitrogen, N) is:

$$\frac{\partial}{\partial t} N + \frac{\partial}{\partial x} (uN) + \frac{\partial}{\partial y} (vN) = f_N \qquad (9)$$

where f_N is the rate of formation (or depletion) of N, and u and v are components of the velocity field calculated from the circulation model. N is the depth-averaged concentration of nitrogen and is a function of time, t, and horizontal location (x,y).

For a kelp farm with an annual yield of 100,000 dry ash-free tons (DAFT), the annual nitrogen uptake required to sustain production is 3,000 tons, assuming 1.8% N dry weight content in the kelp plant and 40% ash dry weight content of plant solids. If only 60% of the available nitrogen is

actually assimilated by the kelp biomass, the total amount of N required to be available for uptake is 5,000 tons. (Note: the above specifications are based on the GE conceptual design study.) For a 10 km × 1 km farm, the daily N uptake is 6.85 μg-at/L, i.e.:

$$f_N = -6.85 \text{ μg-at/L-day} \tag{10}$$

We analyzed the case in which the fertilizer is applied uniformly over the farm once every week, and the background nutrient concentration is assumed to be negligible. Thus, the initial condition (t = 0) for Eq. 9 is:

$$N_0 = \begin{cases} 48 \text{ μg-at/L, inside the kelp farm} \\ 0, \text{ otherwise} \end{cases} \tag{11}$$

Numerical solution of Eqs. 9-11 is based on a zero-average-phase-error technique (Fromm, 1968).

The nutrient transport model was applied to the 10 km × 1 km farm with the uptake rate, f_N, and initial nutrient condition, N_0, described above; the basic circulation conditions of Section 2 ($\beta = 1$); and an incoming ambient coastal current of 5 cm/s. A time history of the spatial distribution of the concentration of N is shown in Fig. 3 in 28-hr increments. In stagnant water, the N concentration will decrease to zero over a one-week period due to uptake alone. However, due to advection, the nutrient concentration decreases more rapidly in the kelp farm. Also, the farm "effluents" with a concentration comparable to the initial N concentration are confined to a narrow (<0.5 km wide) strip; the area is bounded laterally by streamlines enclosing the kelp farm. The downstream extent of the farm "effluents" reflects stretching due to differential advection in and around the farm.

The uptake of applied N by the kelp in the farm is an output of the model, and the uptake by the farm as a percentage of fertilizer applied is shown in Fig. 4 as a function of time for three different scenarios. For the base case of a 10 km × 1 km farm fertilized once a week with a 5 cm/s ambient current (N distributions shown in Fig. 3), 47% of the applied fertilizer is taken up by the kelp in one week (168 hr). Most of the N uptake occurs during the first half of the week, before the higher concentrations of N are transported downstream.

The percentage uptake of applied fertilizer decreases with increased ambient currents (which transport nutrients away from the kelp farm more quickly) and with higher initial N concentration (such as would result from applying two weeks' worth of fertilizer to the farm at once). This is demonstrated in Fig. 4, which shows that, for the 10 km × 1 km farm considered above, increasing the ambient current from 5 cm/s to 10 cm/s results in an uptake of applied fertilizer of only 26% by the end of one week. The doubling of the ambient current magnitude is analogous to increasing the fertilizing interval from one week to two weeks while holding the monthly amount of

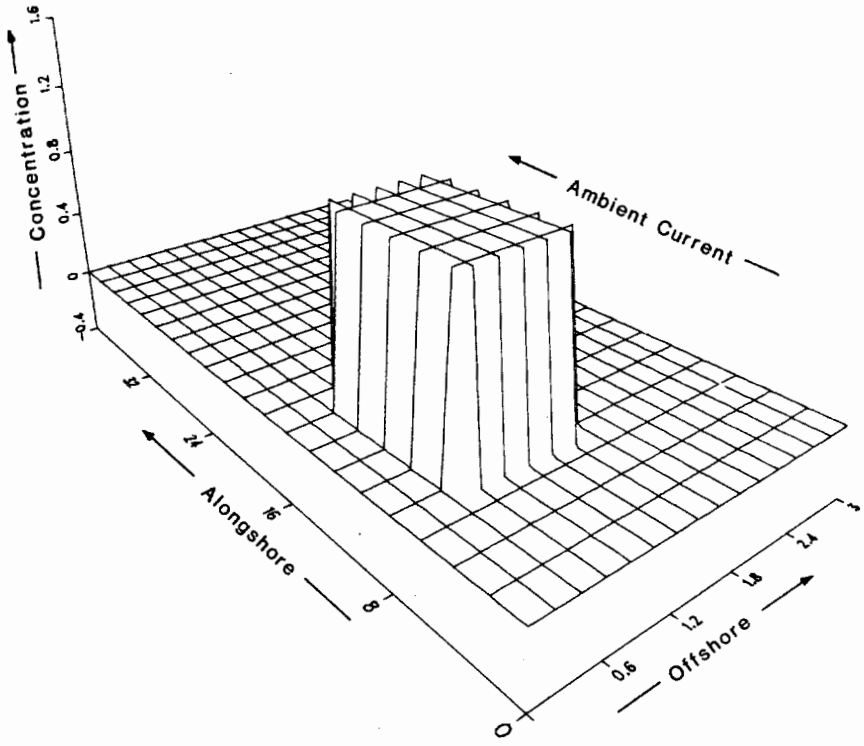

a. t = 0 hr

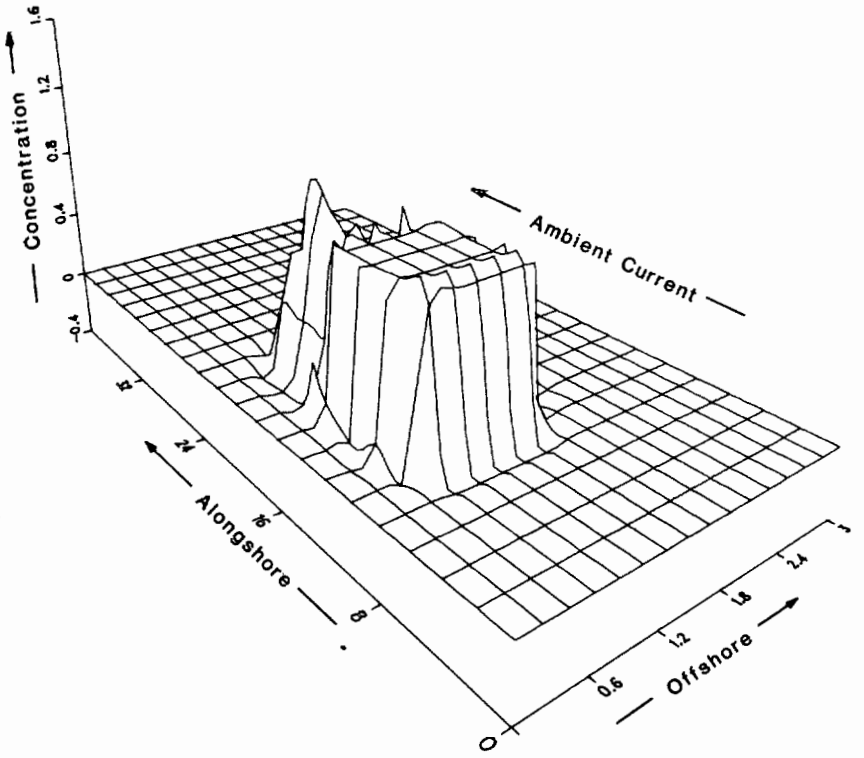

b. t = 28 hr

Fig. 3 Time Sequence of N Concentration for 10 km × 1 km Kelp Farm Covered Uniformly with Fertilizer at t = 0 (ambient current is 5 cm/s, distance scales in km, N concentration normalized with initial concentration)

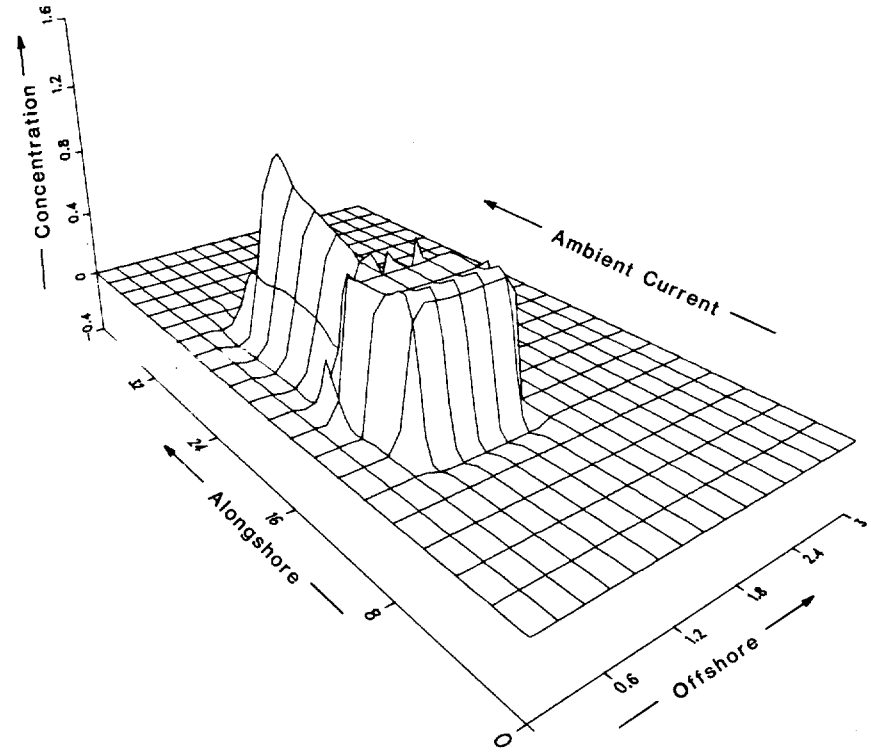

c. t = 56 hr

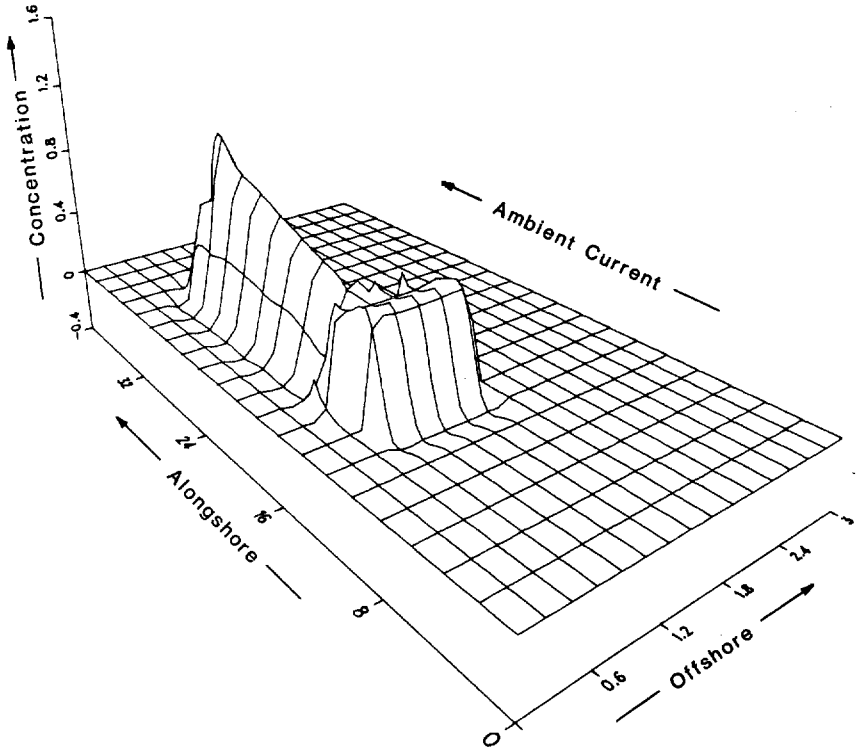

t = 84 hr

Fig. 3 Cont'd

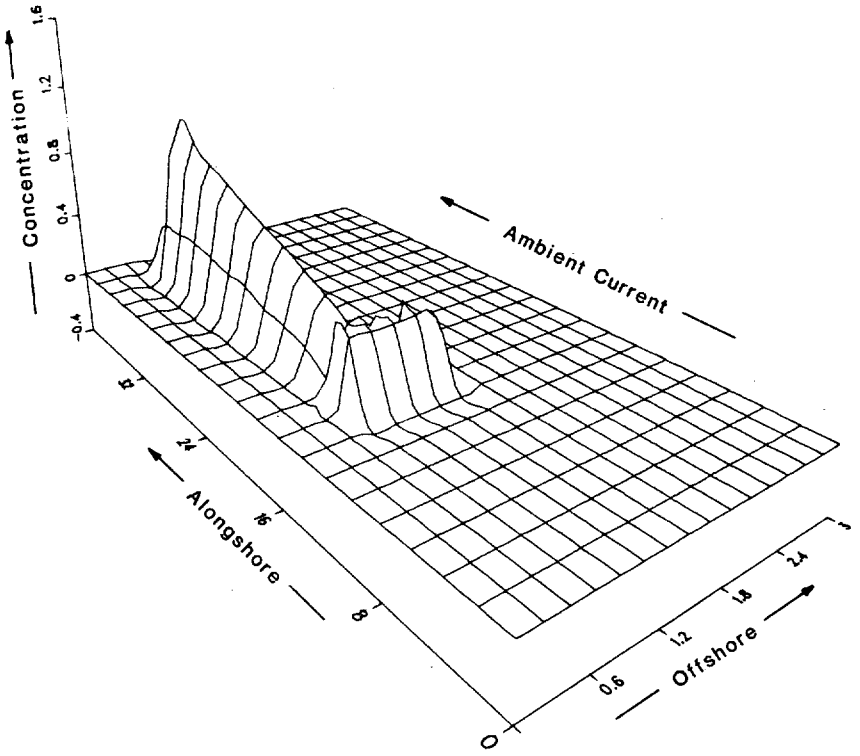

e. t = 112 hr

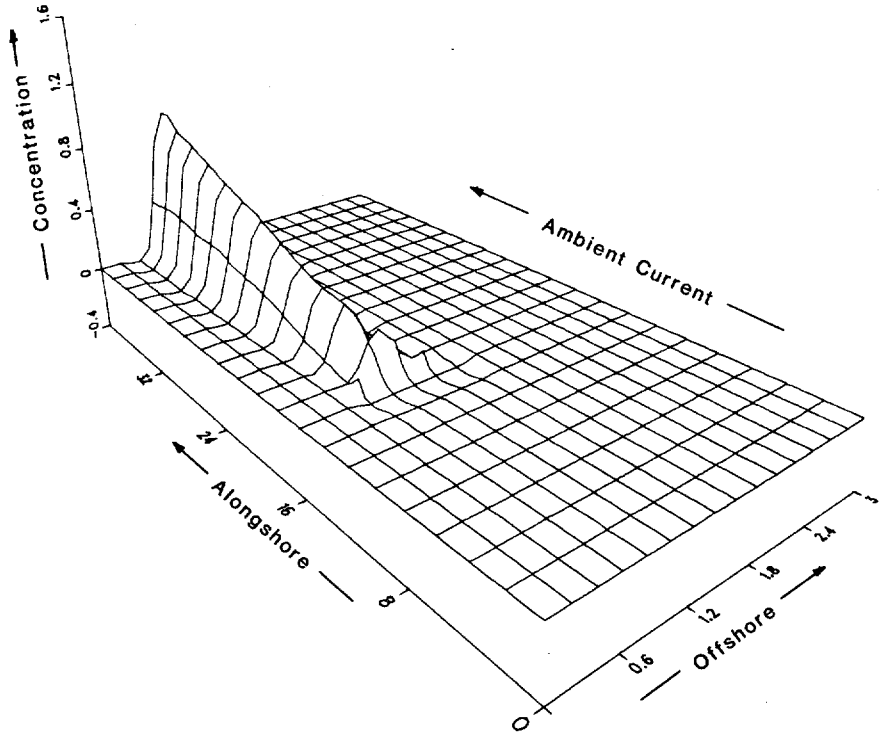

f. t = 140 hr

Fig. 3 Cont'd

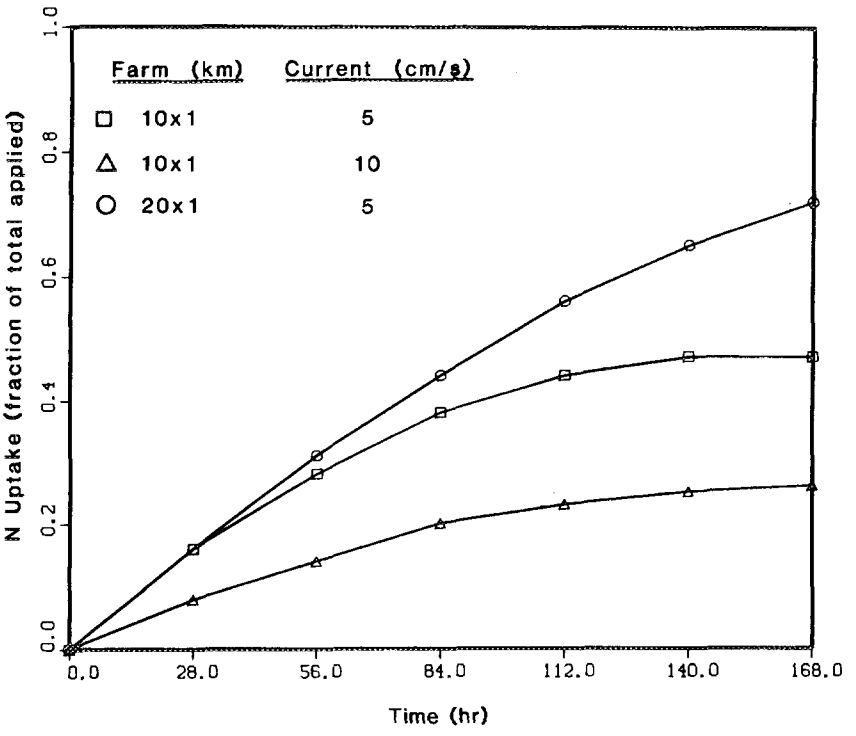

Fig. 4 Time History of Fertilizer Uptake within Kelp Farm as Fraction of N Applied to Farm Once a Week, for Three Farm Size and Ambient Current Combinations

fertilizer constant. For the case of the lengthened fertilizing interval, the time scale is also doubled, that is, the uptake is 26% at the end of two weeks.

For a 20 km × 1 km farm to sustain an annual yield of 100,000 DAFT, the daily N uptake required is 3.43 μg-at/L (the corresponding unit annual yield is 20 DAFT/acre). If the fertilizer is applied once every week and the background nutrient concentration is negligible, the resulting N uptake is similar to that in the smaller farm case. However, for the same ambient current, the residence time is longer in a larger farm, and hence the available nutrient concentrations will be higher. This is shown in Fig. 4, where, for a 5 cm/s inflow, the N uptake by the kelp in one week in a 20 km × 1 km farm is 72% of the total fertilizer applied.

By accounting for the inefficient uptake of nitrogen applied to the farm due to the effects of currents, one can determine the total amount of nitrogen required to produce a specified kelp yield. For the case of a desired annual yield of 100,000 DAFT, a depth-averaged ocean current of 5 cm/s, and fertilizer applied once every week, the annual nitrogen requirements are 10,640 tons for a 10 km × 1 km farm and 6,940 tons for a 20 km × 1 km farm. Of course, the amount of nitrogen supplied as chemical fertilizer can be reduced if some nitrogen is provided from natural nutrients in the ambient

water and/or from methane process plant effluents applied to the farm. Fertilization scenarios involving combinations of nitrogen sources can be examined by modifying the initial conditions and depletion rate terms in the nutrient transport model.

In summary, our analysis indicates substantial loss of fertilizer by advection. Depending on the ambient current, farm size, and fertilization scheme, 30-80% of the fertilizer may be lost. Also, the effluent has a high N concentration, which could significantly affect the downstream environment through potential modifications to the planktonic assemblage and related natural food web leading to fish (Ritschard et al., 1981).

While assessing the magnitude of the environmental effects involves site-specific marine biochemical information, some general observations can be made. The plume downstream of the farm will contain nutrient concentrations well in excess of the concentrations in the ambient surface waters. The farm effluent plume will also probably contain phytoplankton in concentrations about equal to those in the ambient surface waters. Thus, if a nutrient such as nitrogen is limiting crop size and growth rate, enhancement of nitrogen concentrations may stimulate phytoplankton growth in the downstream plume from the farm.

To maximize farm yield and to minimize downstream influence, the advective effects must be considered in the design of a fertilizer distribution scheme. In particular, for given ambient ocean currents and farm unit yield, the farm size and fertilizing interval will significantly affect the nutrient availability.

In the model analysis, we assumed that nutrients are distributed uniformly and that plant uptake of nutrients is uniform through the water column. However, in reality, the plant uptake is most effective near the surface, and the vertical nutrient distribution depends on the fertilization function and ambient density stratification. Thus, our assumption of a homogeneous ocean driven by a depth-averaged current may be overly simplistic. A realistic model should consider the differential advection due to velocity shear, the vertical nutrient distribution, and the depth dependence of nutrient uptake by kelp plants.

Because field data for circulation and transport in a kelp bed are scarce, no attempt was made in this study to compare model prediction with observation. However, the fundamental assumption regarding the relationship between drag force and current is empirical, and the model can be validated only with field data. Direct measurement of currents and bottom pressure is required to test the drag law. The flow field and nutrient transport in the kelp bed can also be determined from tracer measurement.

4 WAVE-FARM INTERACTIONS

The interaction of surface waves with a kelp farm in nearshore coastal waters will modify the waves to which kelp plants are subjected within the farm and will modify the wave field in the vicinity (particularly shoreward) of the farm. Waves propagating into the farm are reduced in height due to the resistance of the kelp plants. The problems of wave height reduction within the farm and the more complex problem of the farm's effects on the local wave climate shoreward of the farm were investigated by COER (see Section II of the Appendix). The results of the investigations are summarized here.

The damping (reduction in wave height) of waves entering the kelp farm was determined by estimating the energy loss, using linear wave theory. The relationship between the incident or incoming wave height, H_1, and the wave height at a distance x into the farm, H(x), is:*

$$\frac{H(x)}{H_1} = \frac{1}{1 + \alpha kx} \tag{12}$$

where:

k = $2\pi/L$ (wave number) and

L = wave length.

The parameter α is a complicated function of the water depth (h), the vertical height of the kelp plant (s), the spacing between adjacent plants (b), the effective diameter of the kelp plants (D), and a drag coefficient (C_D) reflecting both form and skin friction drag.

Equation 12 is plotted in Fig. 2.1 of the Appendix, and Table 2.1 of the Appendix lists values of α for various wave and farm configurations. The procedure to determine values of kx, given water depth and wave period (T), is described as well.

An example calculation for wave height reduction under conditions thought to be relevant to nearshore kelp farms determines the modification to the height of a wave at a location 716 m (2350 ft) into a farm with kelp plants 3 m (10 ft) apart with effective diameters of 0.3 m (1 ft). The water depth and kelp height are 15.2 m (50 ft), the wave period is 20 s, and C_D is assumed to be 1. A wave 6.1 m (20 ft) high outside the farm is 3 m (10 ft) high at a location 716 m into the farm -- a 50% reduction in wave height.

*Equation 12 is identical to Eq. 2.1 in the Appendix.

While the technique described above is rather straightforward to apply, it is limited by the assumption that the farm is infinitely wide (no edge effects) and by the fact that it only treats waves within the farm. To assess the local effects of a finite farm on the wave climate in and around the kelp farm, COER constructed a more sophisticated modeling technique, based on recent modeling developments, that allows for the combined effects of wave refraction (wave height and direction changes due to changing depths) and wave diffraction (changes due to wave height discontinuities caused by the presence of structures).

The refraction-diffraction model was applied by COER for example problems of kelp farms in coastal waters to examine the extent of the zone of wave height reduction behind (shoreward of) the farm. Two examples of waves directly incident on a farm differ in the density (or spacing) of kelp plants and the size of the farm. In the case of plants on 1-m (3.5-ft) centers and a small farm (see Appendix Fig. 2.3), wave heights are reduced to 20% of incident values immediately behind the farm and are still reduced by 60% two or three farm widths away in a "shadow zone" shoreward of the farm. For the case of plants on 3-m (10-ft) centers and a larger farm (see Appendix Fig. 2.4), five to six farm widths (onshore dimension) are required for wave heights to regain 80% of initial heights.

Other example computations indicate that the model performs as one would expect: incident waves at an angle to the farm result in a shadow zone at an angle to the farm (see Appendix Fig. 2.5), decreases in the effective diameter of the kelp result in less wave height reduction and a smaller shadow zone (see Appendix Fig. 2.6), and changing the wave period from 20 s to 10 s has no appreciable effect on the shadow zone (see Appendix Fig. 2.7). The examples indicate that the kelp farm, depending on the wave and farm characteristics, can alter the local wave climate significantly.

5 IMPLICATIONS OF WAVE-FIELD MODIFICATIONS

The most obvious implication of the reduction in wave energy and wave height in and behind (shoreward of) a kelp farm in the nearshore coastal zone is potential shoreline or beach modifications. The transport of sand nearshore and the shoreline bathymetry are governed primarily by the waves reaching the nearshore area. Experience with breakwaters and other structures near the shore has shown that wave shadowing that interrupts sand transport through the littoral zone can cause tombolos (regions of shallow water created by sand moved from nearshore to offshore) to form in the shadow zone.

A model developed recently by COER for other purposes was used in an exploratory way to examine the potential for shoreline modification by nearshore kelp farms. The details of the application are described in Section IV of the Appendix. The wave field resulting from the interaction of a kelp farm and a 6.1-m (20-ft) wave with a 20-s period was found from the refraction-diffraction model and used as input to the sediment-transport/shoreline-modification model for a shoreline 2650 m (8700 ft) behind the farm. Calculations for seven days indicated that the 7.6-m (25-ft) and 10.7-m (35-ft) bottom contours were migrating from shore into the shadow zone behind the farm. Such calculations are preliminary and the modeling of the shoreline modifications is complex, but the COER exploratory work suggests that tools are available to begin to look at such impacts of kelp farms.

Another implication of the reduction of wave height in and around a kelp farm is the modification of the suspended sediment regime, with the potential for increased sediment deposition within the farm area. This problem is rather complex, as indicated in Section V of the Appendix. A model attempting to account for the suspended sediment concentration in a wave field was used to estimate that wave damping might reduce suspended sediment load by about 20% within the farm. The effects of circulation due to current-farm interactions need to be added to this analysis.

6 WAVE FORCES ON KELP PLANTS

The forces exerted on a nearshore kelp farm, and thus on any restraint system for the farm itself, depend on the forces exerted on the kelp plants. The design of plant attachment systems requires a knowledge of the forces on the kelp plants. COER investigated the state of knowledge of the effects of wave forces on kelp plants, and its findings are reported in detail in Section III of the Appendix.

Essentially there are no experimental data on, or analysis of, the forces exerted on flexible objects such as kelp fronds. However, existing knowledge of wave forces on rigid cylindrical bodies and an analysis of the potential displacement of kelp in a wave field provide some information that does not seem to have been taken into account in previous kelp farm design exercises. Until present, drag forces on kelp plants due to steady currents have been employed. Estimates of the additional force component due to wave accelerations of the water (inertial force) by COER suggest that vertical force components, in particular, are of the same order of magnitude as buoyant forces and cannot be ignored in design. Additional horizontal force components appear to be small relative to steady current drag forces.

7 CONCLUSIONS

The analyses and modeling undertaken in this project are initial investigations of many of the problems posed, and the applications of the techniques have been limited in terms of the range of ocean and kelp farm conditions examined. Thus, the conclusions are stated only in the context of the levels of complexity of the analyses employed and of the examples cited. Nonetheless, the examples from which the conclusions result are believed to be in the spectrum of real cases of nearshore kelp farms. The principal conclusions are:

- A kelp farm significantly modifies the flow of nearshore ocean currents. Inside the farm, the flow is retarded to 30-40% of the incoming current. A deflected flow is created that moves around the kelp farm in a narrow band about 1 km wide.

- Substantial amounts of applied fertilizer are lost from a kelp farm by advection (currents within the farm). Depending on the ambient current, farm size, and fertilization scheme, 30-80% of the fertilizer applied may be lost. Also, the effluent (water leaving the farm proper) has a high nutrient concentration that may have significant environmental impacts downstream.

- Wave heights can be significantly reduced as waves propagate into a kelp farm. The amount of the reduction depends on the hydrodynamic and geometric characteristics of the waves and the kelp. A theoretical formulation has been developed for the convenient calculation of this damping.

- A kelp farm disturbs the local wave field. Behind the farm is a shadow area, which is a region of reduced wave heights. The size, particularly the shoreward extent, of this shadow zone is important for coastal processes. A computer model of combined refraction/diffraction for water waves has been developed and tested for prediction of size and location of the shadow zone.

- The shadow zone behind a kelp farm may modify the local shoreline. Preliminary use of a model to calculate this shoreline modification has indicated that sand moves from onshore to offshore behind the farm.

- Wave forces on the kelp can be extreme under circumstances of combined waves and currents. Inertial forces should be included in any wave force calculation, and first-order analyses indicate these forces are of the same order of magnitude as the plant buoyancy.

8 RECOMMENDATIONS

This project has provided insight into several physical aspects of ocean kelp farming for which little knowledge was previously available. The limited scope of the project, however, has meant that many analyses were exploratory and applications were confined to a few examples. Several results indicate that the approaches taken can provide understanding essential to critical problems of kelp farm development. Some of the approaches reported here require further examination and application to become credible tools for the marine biomass community. In general terms, without separating supply and environmental issues, we make the following recommendations:

- Some of the basic hydrodynamics in models developed to analyze circulation (and nutrient distribution) and wave field modification need to be verified against observations in natural kelp beds. Additional analytical and experimental studies of wave forces on kelp plants are necessary.

- Several of the models employed in this study need to be improved to investigate and account for effects that were ignored.

  - More remains to be learned about the effects of currents, kelp plant size, farm configuration, and fertilization schemes on vertical nutrient distributions. We did not investigate vertical nutrient distributions and need to consider vertical features such as depth dependence of nutrient uptake by plants and density stratification.

  - Further improvements are required in models for wave field and shoreline modifications, with particular emphasis on application of the models to typical site conditions.

  - Additional study is required of combined wave and current effects on sedimentation and scour in and around the farm, to determine whether the width (or offshore dimension) of the farm may be limited due to the impact of such processes.

- Studies of many of the physical aspects of ocean kelp farming should be considered as fundamental to the development of rational conceptual designs (and not simply considered to be design studies that can be left to the final stages of a site-specific implementation). For example, nutrient distribution studies should be integrated with biological kelp yield studies in the search for fertilization strategies.

REFERENCES

Fromm, J.E., 1968, *A Method for Reducing Dispersion in Convective Difference Schemes*, J. Computational Physics, *3*:176-189.

General Electric Company, Biomass Program Office, Advanced Energy Department, 1982, *System Functional Requirements and Specification for a Nearshore Kelp to SNG Production Facility: Preliminary Engineering Study*, King of Prussia, Penn.

Leone, J.E., 1980, *Marine Biomass Energy Project*, J. Marine Technology Society, *14*:12-31.

Ritschard, R., V. Berg, and S. Killeen, 1981, *Proceedings of a Workshop on Environment Impacts of Marine Biomass*, Gas Research Institute Report GRI-80/0076.

APPENDIX:
OCEAN ENGINEERING ASPECTS OF COASTAL KELP FARMING

prepared by

Robert A. Dalrymple, Paul A. Hwang, and Marc Perlin
Coastal and Offshore Engineering and Research, Inc.
Newark, Delaware

for

Argonne National Laboratory
Energy and Environmental Systems Division
under Argonne Contract 31-109-38-6868

This appendix is reproduced here as received by Argonne from
Coastal and Offshore Engineering and Research, Inc.

TABLE OF CONTENTS

LIST OF FIGURES

I. Introduction and Summary

Marine biomass and its anaerobic digestion into synthetic natural gas has been studied by the Gas Research Institute and its contractors for a number of years. Recently the aim of their efforts has been to evolve a viable design for a nearshore farm for the cultivation and harvest of giant kelp, Macrocystus pyrifera.

Coastal and Offshore Engineering and Research, Inc. (COER) has served as a sub-contractor to Argonne National Laboratory (ANL) which has been charged with the task of examining the physical oceanographic and ocean engineering aspects of coastal kelp farming. COER's statement of work involved the development of first order analyses for the following areas:

1. wave modification in an around the kelp farm
2. shoreline modification
3. wave force analysis

and 4. the effects of the farm on local sedimentation.

The analyses of these problems are prescribed in subsequent chapters and detailed calculations are presented in appropriate appendices.

The presence of the kelp farm with its densely growing plants results in local wave damping, which means the wave heights within the farm are reduced as well as in the region shoreward of the farm. Behind the farm there is a change in wave direction as well. COER has utilized the state-of-the-art knowledge of combined wave refraction/diffraction with wave damping to develop a computer program to determine the wave field in and around the farm. Graphical output from this program shows that the farm can significantly reduce the wave heights over very large areas.

An examination of the effect of the modified wave climate on the shoreline was carried out using the U.S. Army Coastal Engineering Research Center's shoreline modification model, which was developed for them by COER (Perlin and Dean,

1982). While only one simulation has been carried out (for storm conditions), it is possible to compute annual shoreline changes with the model, and based on the results presented, these effects can be significant. The reduced wave height inshore of the farm results in shoreline sediment deposition and, over long periods of time, the shoreline can bulge seaward towards the farm. The magnitude of this effect is of vital importance, particularly along the California shoreline, where the beaches are a vital resource.

The effect of waves on kelp is important for several reasons. The anchoring system for the plants must be sufficient to resist wave forces and the forces should not be of such a magnitude as to pull the plants apart. A study of the wave forces indicates that the drag forces are the most important of the two forces experienced by the plant, but that the inertia force is of the same order of magnitude as the buoyancy force. We find here that the presence of waves and currents can lead to very high forces on the kelp plants; much higher than 35 lbs per plant.

Finally sedimentation around and in the farm is affected as the wave heights are reduced within the farm and the mean currents are deflected around the farm. This means that sedimentation will be increased within the farm and scour will be increased around the perimeter of the farm. Details of these analyses are discussed in Chapter V.

II. Wave Modification Due to the Kelp Farm

Waves propagating into a region of densely growing kelp are reduced in height. There are two important effects which were studied here. First, the reduction of wave height with distance as the waves propagate into the interior of the farm was studied and then the more complex problem of examining the effect of the farm on the entire local wave climate; that is to determine the effect of the kelp on the waves inside and shoreward of the farm. These two problems are discussed separately below.

1. Wave Damping in the Farm

Energy loss by the waves due to work exerted on the kelp plants can be determined using linear water wave theory. The theoretical derivation is presented in Appendix I. The major determining parameters for the damping rate are the spacing of the plants, b, and their effective hydraulic cross section, D, (the projected area with respect to the flow) and a drag coefficient. Here the drag coefficient, C_D is taken to be a combination of the standard pressure drag coefficient and the skin friction coefficient.

The results of the analysis shows that the wave height decays with distance in the following manner:

$$\frac{H(x)}{H_1} = \frac{1}{1+\alpha kx} \tag{2.1}$$

where H_1 is the wave height entering the farm, x is the distance into the farm and kx is the dimensionless distance into the farm and k is defined as

$$k = \frac{2\pi}{L} \tag{2.2}$$

where L is the water wave length.

Therefore, kx is 2π times the number of wavelengths the wave has propagated into the farm. The factor α is a complicated function of water depth (h), plant spacing and the vertical height of the kelp plants, s.

$$\alpha = \frac{C_D}{3\pi}\left(\frac{D}{b}\right)\left(\frac{H_1}{b}\right)(\sinh^3 ks + 3\sinh ks)\left(\frac{4}{3\sinh kh(\sinh 2kh + 2kh)}\right) \qquad (2.3)$$

With its hyperbolic functions, α, is difficult to compute, so tables of α have been prepared for relevant values of the parameters.

Figure 2.1 shows a plot of H/H_1 versus αkx. For small αkx the damping $(H(x)/H_1)$ is linear with αkx.

$$\frac{H(x)}{H_1} \approx 1 - (\alpha kx) \quad \text{for} \quad \alpha kx \ll 1$$

Table 2.1 presents α for various wave and plant configurations. To use the table and Figure 2.1, the parameters C_D, D, b, s and kh must be known. Of these, kh is related strictly to the wave conditions. To find kh, the water depth, h, and wave period, (T), of the wave must be known. The kh follow by solving the following transcendental equation for kh.

$$\left(\frac{2\pi}{T}\right)h^2 = g(kh)\tanh(kh) \qquad (2.4)$$

This is most readily done by a Newton-Raphson iterative procedure, see Appendix I. With these parameters selected then α is obtained from the table. (To find kx, it is only necessary to multiply kh by (x/h).)

EXAMPLE: Find the wave height at a distance of 2350 ft into the farm. Given - $C_D = 1$, $D = 1'$, $b = 10'$, $H_1 = 20'$, $s = h = 50'$, $T = 20$ s. Solving Equation (2.4), kh = .40.

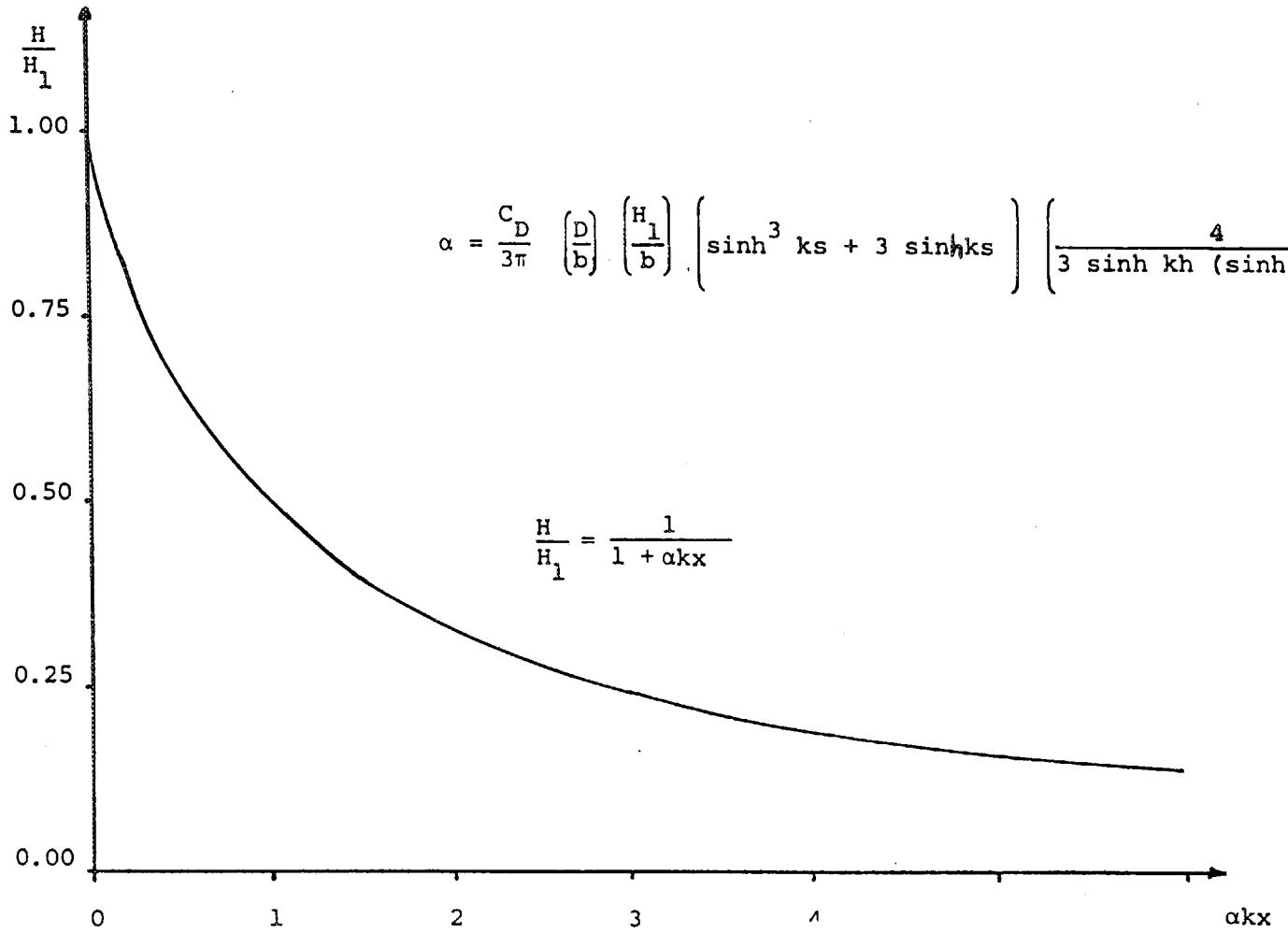

FIGURE 2.1 Wave Attenuation With Dimensionless Distance, αkx, Into Kelp Farm

TABLE 2.1

*** KELP DAMPING FACTOR (ALPHA) ***

(a) C_D D/B: 0.100, s/h = 1.000

kh\H/B	3.000	6.000	9.000	12.000	15.000	18.000	21.000
0.10	0.3183	0.6366	0.9549	1.2732	1.5916	1.9099	2.2282
0.20	0.1592	0.3183	0.4775	0.6367	0.7958	0.9550	1.1142
0.30	0.1061	0.2123	0.3184	0.4246	0.5307	0.6368	0.7430
0.40	0.0797	0.1593	0.2390	0.3187	0.3983	0.4780	0.5577
0.50	0.0638	0.1277	0.1915	0.2553	0.3192	0.3830	0.4468
0.60	0.0533	0.1067	0.1600	0.2134	0.2667	0.3200	0.3734
0.70	0.0459	0.0918	0.1378	0.1837	0.2296	0.2755	0.3215
0.80	0.0404	0.0809	0.1213	0.1618	0.2022	0.2427	0.2831
0.90	0.0363	0.0726	0.1088	0.1451	0.1814	0.2177	0.2540
1.00	0.0330	0.0661	0.0991	0.1322	0.1652	0.1983	0.2313

(b) C_D D/B: 0.100, s/h = 0.500

0.10	0.1586	0.3171	0.4757	0.6342	0.7928	0.9514	1.1099
0.20	0.0784	0.1568	0.2352	0.3136	0.3920	0.4704	0.5487
0.30	0.0513	0.1026	0.1539	0.2052	0.2565	0.3077	0.3590
0.40	0.0375	0.0749	0.1124	0.1499	0.1873	0.2248	0.2623
0.50	0.0290	0.0580	0.0869	0.1159	0.1449	0.1739	0.2029
0.60	0.0232	0.0463	0.0695	0.0927	0.1159	0.1390	0.1622
0.70	0.0189	0.0378	0.0567	0.0757	0.0946	0.1135	0.1324
0.80	0.0156	0.0313	0.0469	0.0626	0.0782	0.0939	0.1095
0.90	0.0130	0.0261	0.0391	0.0522	0.0652	0.0783	0.0913
1.00	0.0109	0.0219	0.0328	0.0438	0.0547	0.0656	0.0766

(c) C_DD/B: 0.200, s/h = 1.000

0.10	0.6366	1.2732	1.9099	2.5465	3.1831	3.8197	4.4564
0.20	0.3183	0.6367	0.9550	1.2733	1.5917	1.9100	2.2283
0.30	0.2123	0.4246	0.6368	0.8491	1.0614	1.2737	1.4860
0.40	0.1593	0.3187	0.4780	0.6373	0.7967	0.9560	1.1153
0.50	0.1277	0.2553	0.3830	0.5107	0.6383	0.7660	0.8937
0.60	0.1067	0.2134	0.3200	0.4267	0.5334	0.6401	0.7468
0.70	0.0918	0.1837	0.2755	0.3674	0.4592	0.5511	0.6429
0.80	0.0809	0.1618	0.2427	0.3236	0.4045	0.4854	0.5663
0.90	0.0726	0.1451	0.2177	0.2902	0.3628	0.4354	0.5079
1.00	0.0661	0.1322	0.1983	0.2644	0.3304	0.3965	0.4626

(d) C_DD/B: 0.200, s/h = 0.500

0.10	0.3171	0.6342	0.9514	1.2685	1.5856	1.9027	2.2198
0.20	0.1568	0.3136	0.4704	0.6271	0.7839	0.9407	1.0975
0.30	0.1026	0.2052	0.3077	0.4103	0.5129	0.6155	0.7181
0.40	0.0749	0.1499	0.2248	0.2998	0.3747	0.4496	0.5246
0.50	0.0580	0.1159	0.1739	0.2318	0.2898	0.3478	0.4057
0.60	0.0463	0.0927	0.1390	0.1854	0.2317	0.2781	0.3244
0.70	0.0378	0.0757	0.1135	0.1513	0.1892	0.2270	0.2648
0.80	0.0313	0.0626	0.0939	0.1252	0.1565	0.1877	0.2190
0.90	0.0261	0.0522	0.0783	0.1044	0.1305	0.1566	0.1827
1.00	0.0219	0.0438	0.0656	0.0875	0.1094	0.1313	0.1532

The factor $C_D D/b = 0.1$ and $(s/h) = 1$, therefore, we use Table 2.1.a. The corresponding α value is 0.0531. Therefore, $\alpha kx = (0.0531)(0.40)(\frac{2350}{50}) = 0.998$. Now, using Figure 2.1, we find $H/H_1 = 0.5$ for this value of αkx. Therefore, the wave height 2335' into the farm is 10', a reduction of 50%.

To eliminate the necessity of calculating α for a particular case and to show the effect of s, the fraction of the water column over which the kelp extends, Figure 2.2 shows H/H_1 versus kx for T = 20 seconds, h = 50', D = 1', b = 10', $C_d = 1.0$ and the following values of s/h: 1.0 (Curve 1), 0.8 (2), 0.6 (3), 0.4 (4), 0.2 (5). Similar curves for other parameters can easily be generated using Equation (2.3) for α and Equation (2.1).

2. Wave Climate Modification in and Around the Farm

The model presented above strictly examines the waves propagating into a farm of infinite width, that is, there is no effect of the lateral edges of the farm and no consideration of the waves after propagating through the farm. Since the kelp farm can be considered conceptually as a very porous offshore breakwater, it is necessary to determine its effects on the adjacent shorelines. (Rubble mound offshore breakwaters are often used as a coastal engineering method to disrupt the longshore sediment transport in order to create deposits of sand behind the breakwater for recreational beaches.)

To this end, the effect of the farm on the local wave field was calculated using a recently developed technique for combined wave refraction (wave height and direction changes for changing depths) and diffraction

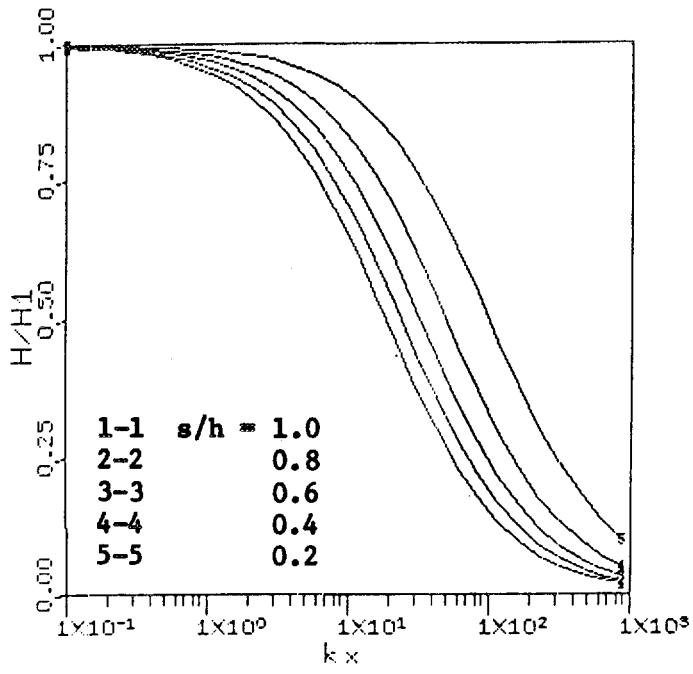

FIGURE 2.2 Wave Attenuation With Dimensionless Distance (kx) Into Kelp Farm (C_D = 1.0, b = 10', H = 20', D = 1')

(changes due to wave height discontinuities due to the presence of structures). This technique due to Radder (1979) and Booij (1981) and is referred to as the parabolic model. The theoretical developments and computational implementation are discussed in Appendix II. In this section the results of the model will be presented graphically. Due to spatial limitations of the graphical software, a small farm [2,000' long (longshore) and 1,000' wide (onshore] was chosen for the first example to show the far field effect of the farm. In Figure 2.3, the kelp farm is located in the center of the upper right hand side of each diagram and the waves are incident on the farm from that direction. The bottom diagram shows the waves at an instant of time as they occur around and in the farm. The upper diagram shows transmission coefficient, K_T - ($\equiv H/H_1$) at all times. As can be seen from the K_T diagram the wave heights for this case of strong damping[1] the wave heights leaving the farm are less than 20% of the incident wave height. At a distance of 2 or 3 farm widths behind the farm the $K_T = 0.4$ contour closes. This means, in this case, that 4,000-6,000 ft shoreward of the farm, the waves are still reduced by 60%. At extremely large distances behind the farm, it is expected that $K_T = 1.0$. An interesting effect, visible in the figure, is the appearance of a bow wave-like phenomena, which creates the wave height highs which trail off behind the front edge of the farm at an angle of about 10°.

The next figure, Figure 2.4, shows a larger kelp farm exposed to the same wave conditions except that the plant spacing is measured to a more realistic 10'. The kelp farm is 9,600' long and 3,000' wide. The plotted coastal region is 24,000' x 12,000'. For this case the wave height is reduced to less than 40% of the initial 20' height behind the farm and the diffraction process then causes the heights to recover behind the farm. It is estimated

---

[1] $C_D = 1.0$, $D = 1$, $b = 3.5$.

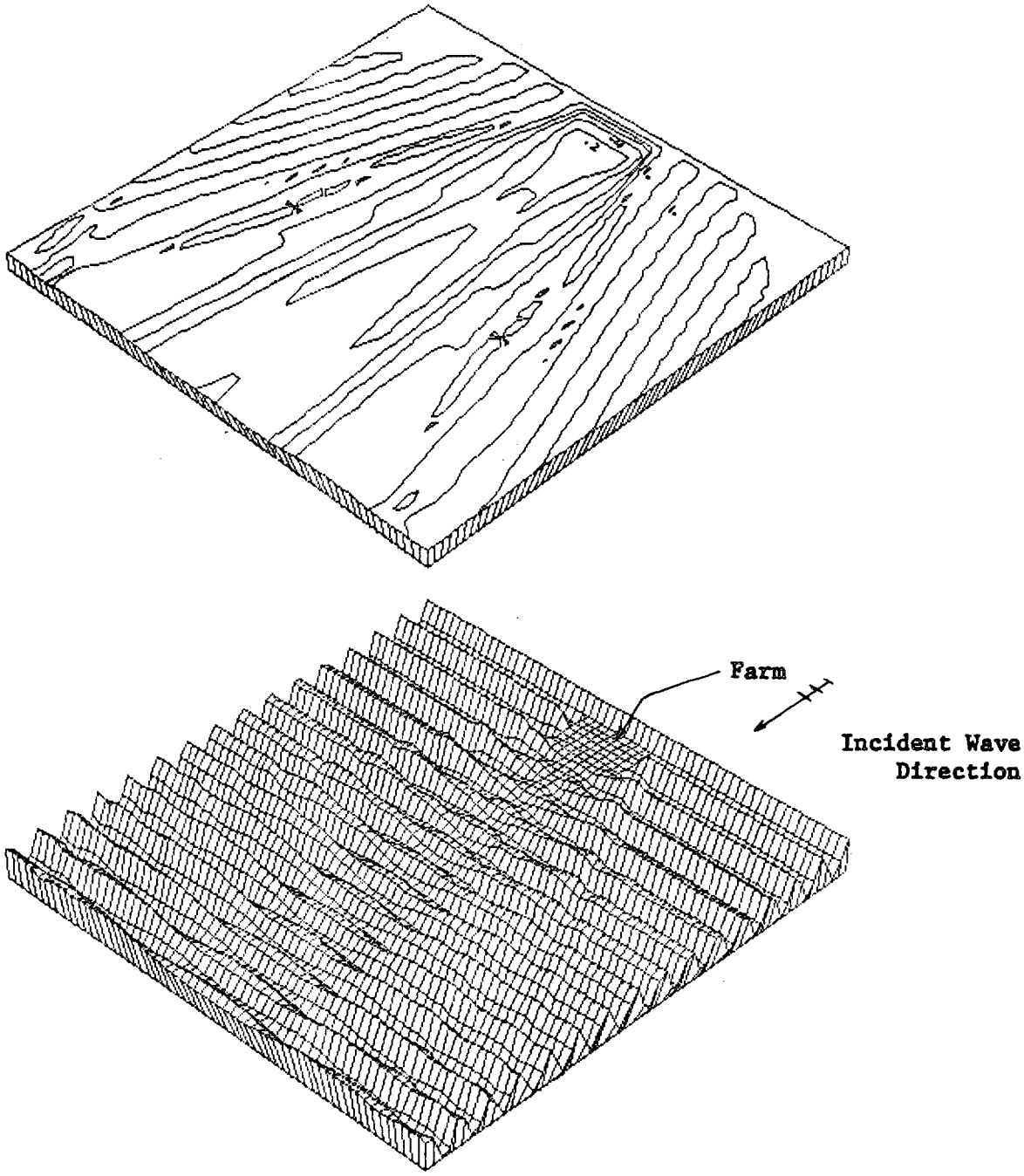


```
LEGEND:
NUMERICAL M=  60,N=  60,DX= 200.0,DY= 200.0,B.C. CODE= 2
WAVE: T= 20.0,DPT REF= 50.00,L REF= 781.95,H REF= 20.00,THETA=  0.00
BOTTOM CODE: 0,SLOPE OR A VALUE= 0.00000
KELP: ELV/DPT=1.0,DIA=1.0,SPACING=   3.50 ,FARM LENGTH-Y (GRID)= 10,WIDTH=  5
 F DAMP=  1.000
PLOTTED FROM (UPPER LEFT CORNER):   1   1 PLOTTED SIZE (X BY Y):  60  60
#?
#ET=7:53.5 PT=17.4 IO=32.4
```

FIGURE 2.3 Wave Field In and Around Kelp Farm: Strong Damping. Top Figure Shows Wave Amplitude and the Bottom Figure Shows the Waves at One Instant.

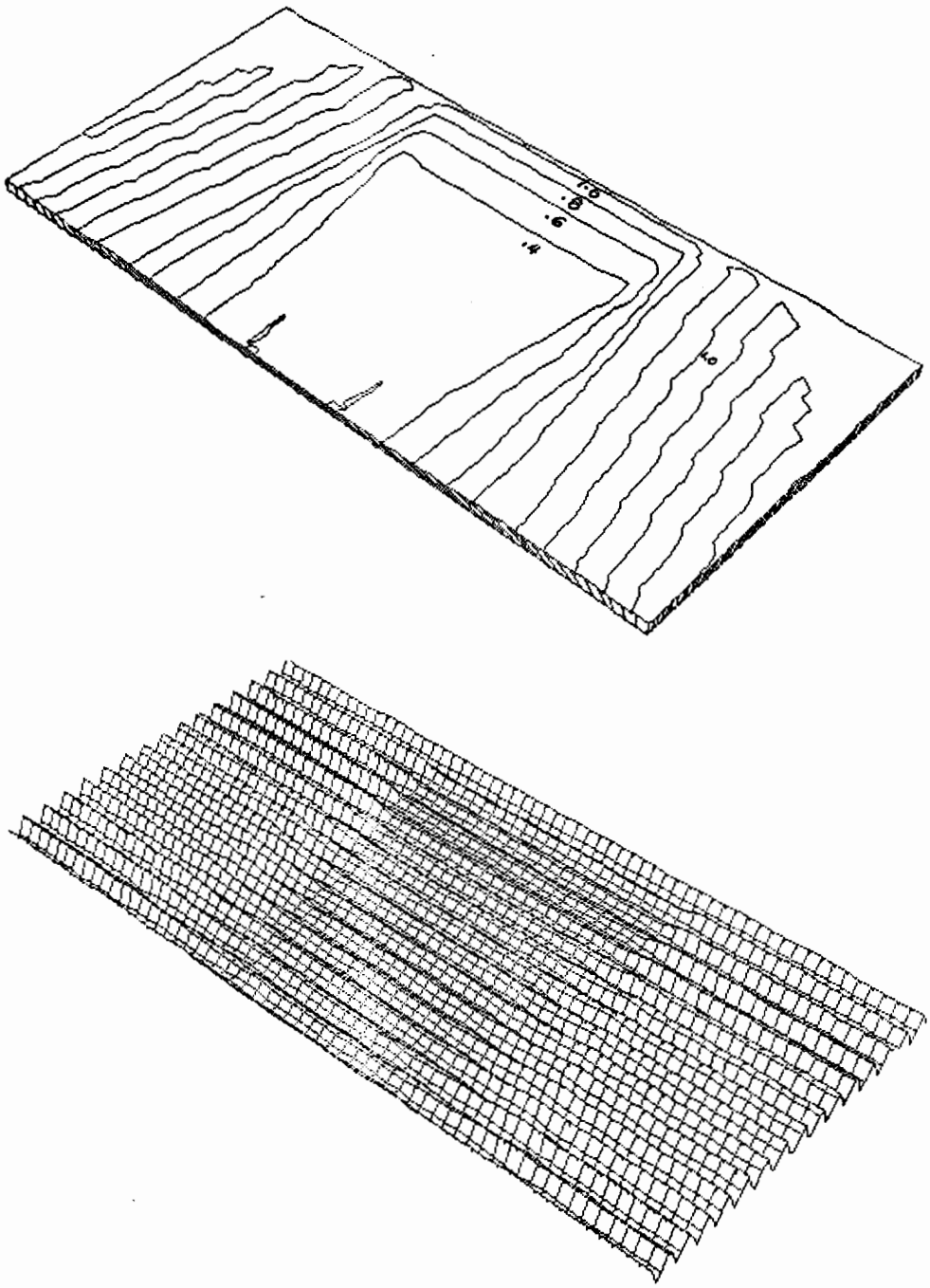


```
LEGEND:
NUMERICAL M=  60,N=  60,DX= 200.0,DY= 400.0,B.C. CODE= 2
WAVE: T= 20.0,DPT REF= 50.00,L REF= 781.95,H REF= 20.00,THETA=  0.00
BOTTOM CODE: 0,SLOPE OR A VALUE= 0.00000
KELP: ELV/DPT=1.0,DIA=1.0,SPACING=  10.00,FARM LENGTH-Y (GRID)= 24,WIDTH= 15
 F DAMP=  1.0000
PLOTTED FROM (UPPER LEFT CORNER):   1   1 PLOTTED SIZE (X BY Y):  60  60
#?
#ET=8:04.7 PT=11.6 IO=31.9
```

FIGURE 2.4 Wave Field in and Around Kelp Farm: Design Conditions

that 5-6 farm widths are necessary before the wave heights recover to 80% of the initial height for this case.

The effect of incident wave angle is shown in Figure 2.5. As can be seen, the shadow region (region of reduced wave height) is directed behind the farm at the same 30° angle. For a farm located in a region of variable angles of wave incidence, the shadow zone will respond directly to the incident wave angle. This will tend to smooth out the effect of the farm on the adjacent shoreline.

For Figure 2.6, the hydraulic diameter of the kelp, D, was reduced to 0.5' from the 1' used previously. Clearly for this case, the wave height reduction is less (the wave height leaving the farm is just below 60% of the incident height).

To illustrate the effect of wave period, a 10 second wave (instead of 20 second) was used in Figure 2.7. Due to the change in period, the computational grid size was also reduced. The farm remains the same size but only half the surrounding area is shown. In comparing this figure to Figure 2.5 (for T = 20), there is no appreciable difference in wave damping for this case, although in general it is expected the damping will decrease with wave period.

Clearly, the results of the combined refraction/diffraction model show that the kelp farm, depending on the values of the wave force parameters and plant characteristics, can significantly alter the local wave climate. This effect persists far behind the farm and could create a significant modification of the shoreline.

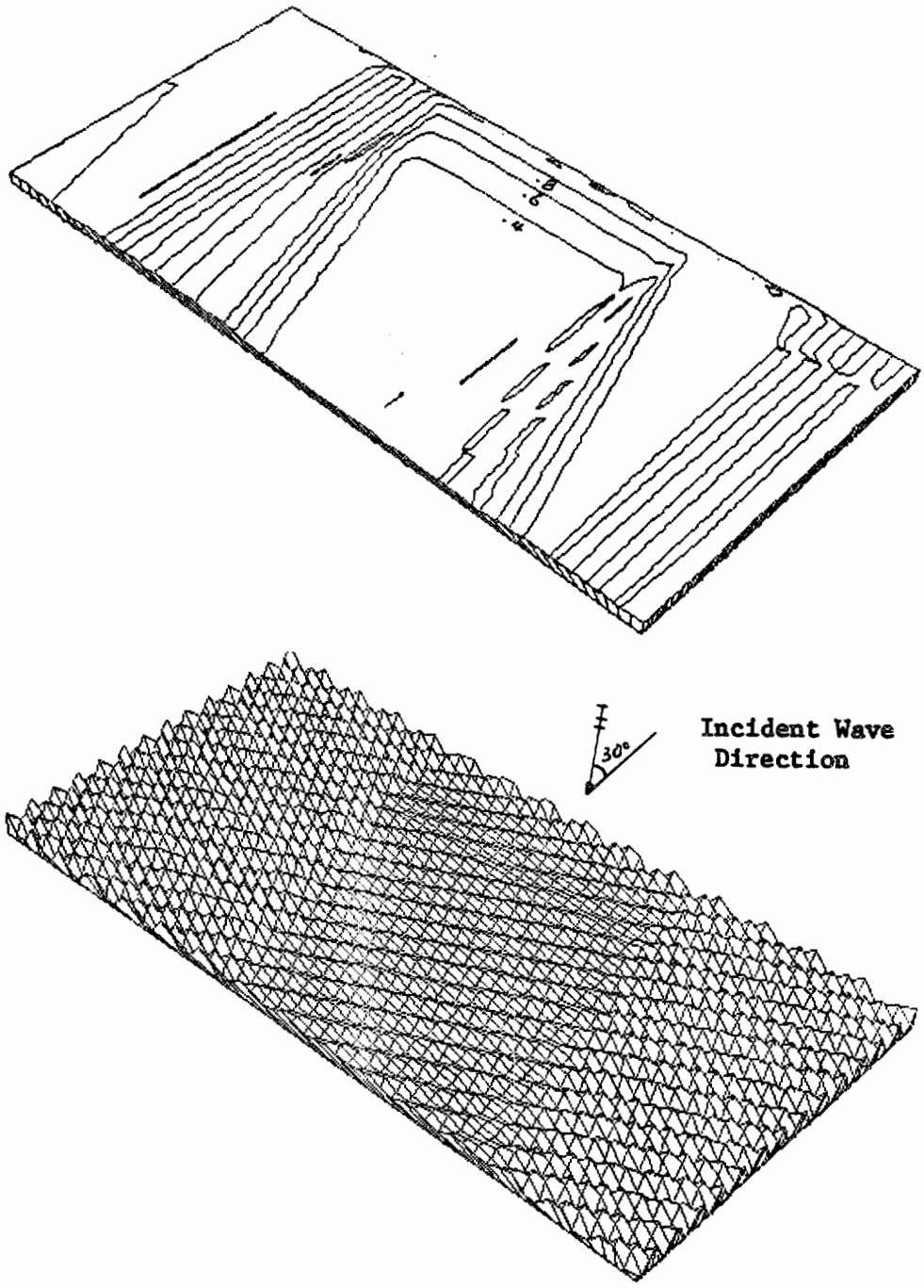


```
LEGEND:
NUMERICAL M=  60,N=  60,DX= 200.0,DY= 400.0,B.C. CODE= 2
WAVE: T= 20.0,DPT REF= 50.00,L REF= 781.95,H REF= 20.00,THETA= 30.00
BOTTOM CODE: 0,SLOPE OR A VALUE= 0.00000
KELP: ELV/DPT=1.0,DIA=1.0,SPACING=  10.00,FARM LENGTH-Y (GRID)= 24,WIDTH= 15
 F DAMP=  1.0000
PLOTTED FROM (UPPER LEFT CORNER):   1   1 PLOTTED SIZE (X BY Y):  60  60
#?
#ET=11:59.6 PT=19.1 IO=31.3
```

FIGURE 2.5 Wave Field In and Around Kelp Farm: 30° Oblique Incidence

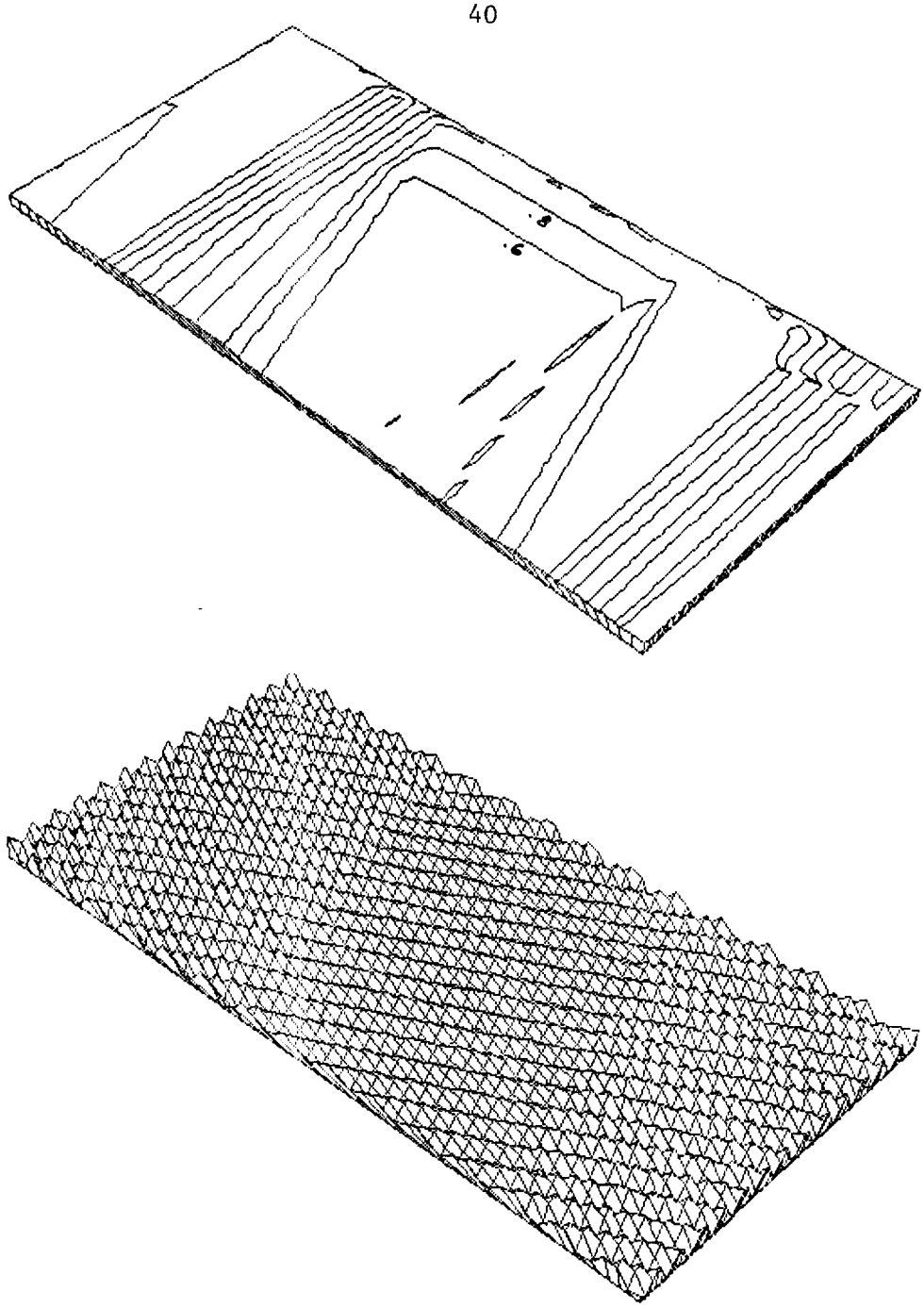

LEGEND:
NUMERICAL M= 60,N= 60,DX= 200.0,DY= 400.0,B.C. CODE= 2
WAVE: T= 20.0,DPT REF= 50.00,L REF= 781.95,H REF= 20.00,THETA= 30.00
BOTTOM CODE: 0,SLOPE OR A VALUE= 0.00000
KELP: ELV/DPT=1.0,DIA=0.5,SPACING= 10.00,FARM LENGTH-Y (GRID)= 24,WIDTH= 15
F DAMP= 1.0000
PLOTTED FROM (UPPER LEFT CORNER): 1 1 PLOTTED SIZE (X BY Y): 60 60
#?
#ET=16:42.5 PT=19.4 IO=32.3

FIGURE 2.6 Wave Field In and Around Kelp Farm: Smaller D.

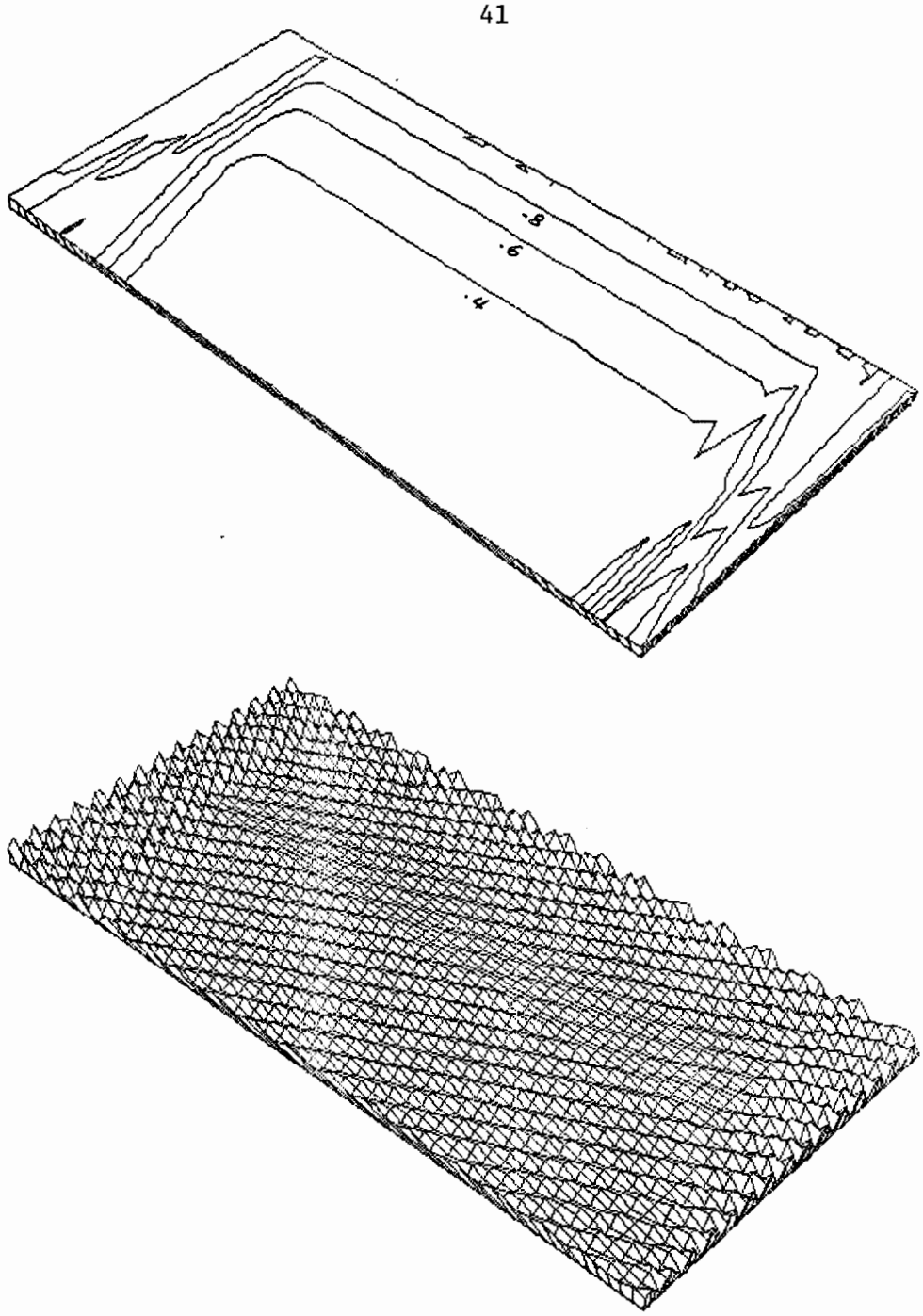


```
LEGEND:
NUMERICAL M=  60,N=  60,DX= 100.0,DY= 200.0,B.C. CODE= 2
WAVE: T= 10.0,DPT REF= 50.00,L REF= 360.08,H REF= 20.00,THETA= 30.00
BOTTOM CODE: 0,SLOPE OR A VALUE= 0.00000
KELP: ELV/DPT=1.0,DIA=1.0,SPACING=  10.00,FARM LENGTH-Y (GRID)= 48,WIDTH= 30
 F DAMP=  1.0000
PLOTTED FROM (UPPER LEFT CORNER):   1   1 PLOTTED SIZE (X BY Y):  60  60
#?
#ET=10:36.3 PT=20.2 IO=36.7
```

FIGURE 2.7 Wave Field In and Around Kelp Farm: 10 Second Period

III. Wave Forces on Kelp Plants

Wave forces on individual kelp plants are very difficult to calculate as the prior experience of engineers has been largely related to rigid cylindrical structures which are of utmost concern to the oil industry. The kelp behaves in a far different manner than a cylindrical pile, in part because it is flexible and able to follow the motion of the water easily and because the fronds are able to stream out behind the plant which streamline the plant to the flow.

The forces exerted by waves on objects consists of two parts, the drag force (per unit length), F_D, and the inertial force (per unit length), F_I, (Morison, et al., 1950). The total force, F_T, is then the sum of these forces. Therefore,

$$F_T = F_D + F_I \tag{3.1}$$

where $F_D = 1/2\ \rho\ C_D\ A_p\ |u|u + [\frac{C_f}{2} \rho\ A_L\ |u|u]$

and $F_I = C_m\ \rho\ \forall \frac{Du}{Dt}$

F_D is composed of two types of drag, the form drag, due to pressure differences upstream and downstream of an object, and the skin friction. Here A_p is the projected area, A_L is the surface area (one side) of the kelp frond. $\forall$ is the volume per unit length of the kelp plant and C_m is the inertial coefficient which can be taken to be about 1.2.

G.E. (1982, see also McGinn, 1981) has discussed in detail the drag force due to a steady current, and some evidence is presented to validate the formula. For large currents, about 2 kts., the plants respond by heeling over to about 83% from the vertical, hence presenting very little projected area and so most of the force is due to skin friction. For this case, the GE-determined drag force for a 1500' frond length plant surrounded entirely by moving water

is 50 lbs.

To this force loading due to a current, the influence of the wave motion must be included. Using the stream function wave theory (Dean, 1965), the most accurate nonlinear theory available, near bottom velocities for a 20' high, 20 second period wave in 50 feet of water is about 8.3 feet per second (fps). The addition of a 2 kt current results in a total horizontal velocity of about 12 fps. If we nonconservatively assume that only half of the drag force should be used (since the kelp is streaming parallel to the bottom and most of the flow could be on the top half of the plant, the G.E. drag equation yields 250 lbs horizontal force.

To the steady drag force must be added the forces due to the to and fro motion of the waves. To examine these forces it is first useful to examine the extent to which the water particles move. From the linear wave theory (the easiest to use for wave calculations, but not as accurate as the stream function theory), the horizontal displacement of the water under the passage of a wave is given as A_H:

$$A_H = H \frac{\cosh k(h+z)}{\sinh kh} \tag{3.2}$$

where H is the wave height, h is the water depth. For a wave period of 20 seconds and h = 50 ft, the maximum excursion of a water particle is 52 ft. This occurs at the surface; the corresponding bottom excursion is 24.2 ft. Since the mature kelp plants will in general be of about this length (particularly just after harvesting), it appears that under storm conditions the plants (in the absence of a current) will be moving constantly in response to the waves. For much shorter and smaller waves, which would occur most of the time, the water particle excursions are much less than the plant length and the plant does not reach the totally stretched out shape predicted by the steady current analysis.

For the large waves in the presence of currents the plant will be deflected more in the downstream direction than the upstream side as the drag force will be increased significantly in that direction.[1] As the flow changes to the downstream direction, the plant will stream out to its uniform current configuration, but since the flow is accelerating,larger relative velocities will be experienced than for the steady current case. This extra force is difficult to evaluate analytically.

Finally, we can make some estimates of the inertial force, F_I, which are due to the fluid accelerations. Pressure gradients, which cause the orbital water motions, also act on submerged objects and try to accelerate them as well. Principle variables of interest are the volume of fluid displaced by the plant and the fluid accelerations. The volume of a kelp plant was estimated by the G.E. (1982) estimate of 50 kg dry weight per plant. This corresponds to about 1.7 ft^3 of seawater if the solid portions of the kelp were neutrally buoyant. (The pneumatocysts cause a larger displaced volume, but then the solid parts of the plant are heavier than water; it is presumed these two facts cancel each other.) The fluid accelerations are calculated by linear theory, where the horizontal and vertical accelerations are given by

$$\frac{\partial u}{\partial t} = gak \frac{\cosh(k(h+z))}{\cosh kh} \sin(kx-\sigma t) \tag{3.3a}$$

$$\frac{\partial w}{\partial t} = -gak \frac{\sinh (k(h+z))}{\cosh kh} \cos(kx-\sigma t) \tag{3.3b}$$

for the water surface displacement,(a)(cos(kx-σt)). For a kelp plant in 50 ft

[1] Drag force is a function of the velocity squared. For a small current, U, then the drag force is proportional to $(U+u)^2 = u^2(1+2\ U/u)$, where u is the wave velocity. If, for example, U = 10% of u, then the drag is increased by 20% in the downstream direction.

of water, a 20 ft high wave with a 20 second period results in horizontal and vertical accelerations at the water surface of 2.6 ft/sec^2 and 1.0 ft/sec^2. Using an inertia coefficient, C_m, of 1.5 and ρ = 2.0 slugs/ft^3, yields

$$F_I = 6.6 \text{ lbs} \; ; \; 2.6 \text{ lbs}$$

for the maximum horizontal and vertical forces. If instead of using the 20' storm wave, we use a more typical wave of, say, five foot wave height and 7 second period, then the horizontal inertial forces are reduced to 5.8 lbs, but the vertical force is increased to 5.1 lbs. This is due to the fact that the water particles at the surface must rise up to the height of the wave in a smaller amount of time. Based on these simple calculations, additional forces of the order of 7 lbs (the same as the buoyancy) must be included in the design of the anchors.

IV. Shoreline Modification by the Kelp Farm

The diffracted waves shoreward of the kelp farm will propagate shoreward and result in changes in the nearshore sediment transport patterns and, after some time, changes in the planform shape of the shoreline. In order to develop some feel for the response of the shoreline, the recently developed CERC (U.S. Army Corps of Engineers Coastal Engineering Research Center) shoreline model (Perlin and Dean, 1982) was used in conjunction with the output of the combined refraction/diffraction model of Chapter II.

The CERC model is an n contour-line representation of the nearshore bathymetry, where n is any number (here, n = 8). In the model, the longshore direction is divided into equal segments (Δx apart). Each contour line represents a specified depth and it is allowed to move on or offshore according to the conservation of sediment. For each contour segment, there are two modes of sediment transport, onshore and alongshore, just as occurs in nature. More discussion of the model appears in Appendix III.

For a 20 second period wave, 14.1 high,[1] the response of a neighboring shoreline (8,700' shoreward) was calculated over a duration of three and a half days and seven days, for the purposes of looking at short term coastal response. In an actual design application of this model, a year's time would be simulated using the actual or predicted waves at the site. The seven day calculation used here is to illustrate the use of the model and to indicate its utility.

Most of the shoreline modification due to these large storm waves occurs at the seaward-most contours which are outside the surf zone. The modification here is due to the shadow zone behind the kelp farm, while at the

[1] This is a reduction of the 20' high design wave to the root-mean-square wave height to account for spectral effects.

surf zone diffraction and refraction have removed almost all effects of the offshore farm. Figure 4.1 presents the contour changes for the 25' and 35' contours which were on average 2450' and 4500' offshore. In the figure only half of the farm is presented as the solution is symmetric for the case of normal incidence. In the figure, erosion occurs outside the shadow zone behind the kelp farm and the sediment is moved behind the farm. This occurs for both contour lines. Not a significantly greater change occurs after 7 days and, therefore, these results were not plotted. At the 25' contour line a net accretion of 1.3×10^5 ft^3 occurred. The shoreward contours on the other hand, experienced a net erosion, decreasing from 4×10^4 ft^3 at the 15' contour to only 350 ft^3 at the shoreline. This nearshore erosion is due to the presence of the kelp farm as the initial beach profile was an equilibrium profile. For this example sediment moved from the nearshore to the offshore region behind the farm to begin creating a tombolo. Its form, under the storm wave attack, is two tombolos forming at both ends of the farm, however, after a long period of time, the area between the two tombolos would fill in to make one large tombolo. Without further simulations it is impossible to provide time scales for tombolo formation or the eventual sizes of the tombolo.

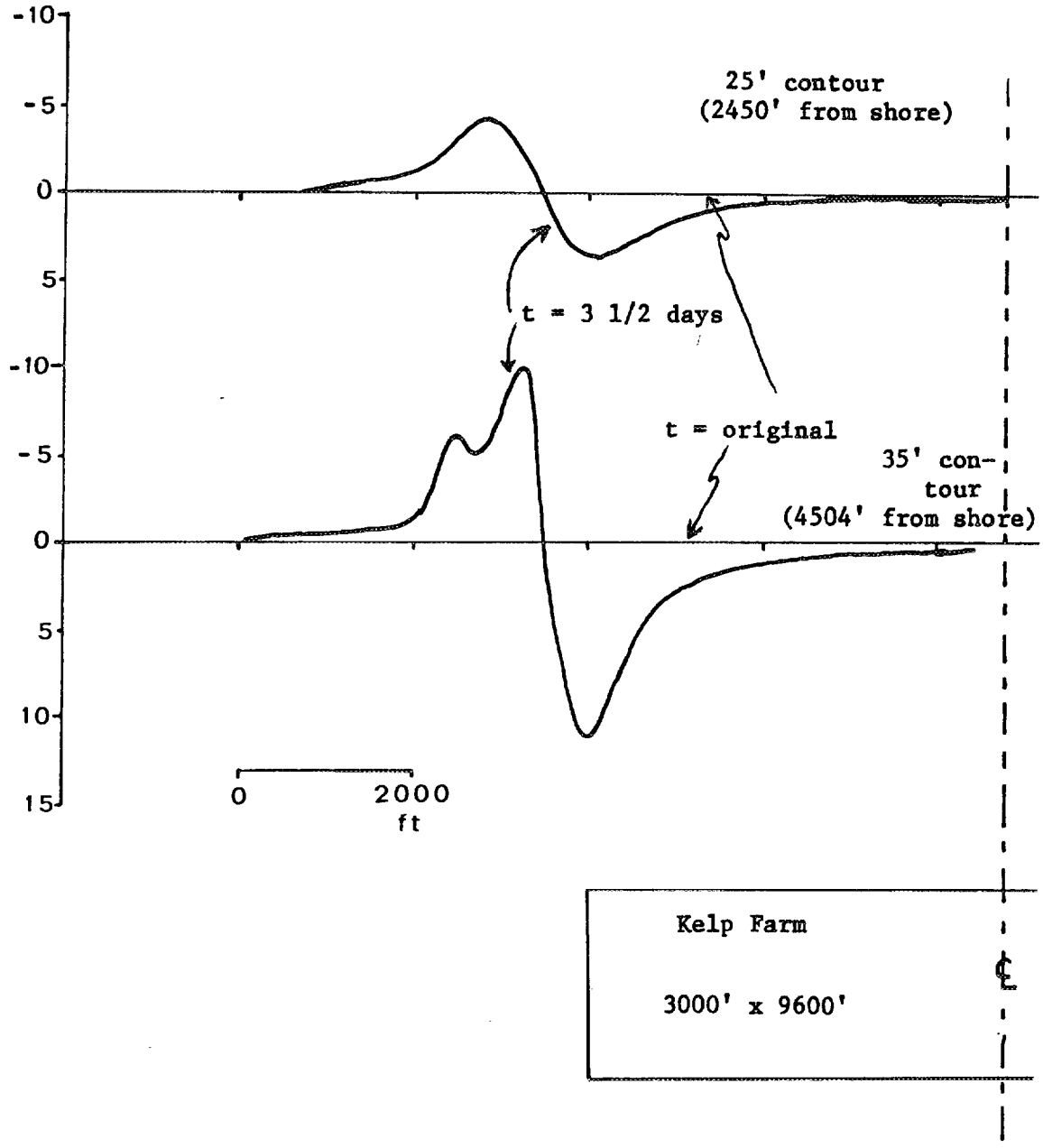

FIGURE 4.1 Bathymetry Changes Due to Diffraction Behind the Farm

V. Sedimentation and Scour Due to the Kelp Farm

In coastal areas a tremendous amount of sediment and biological material is transported by suspension. The sediments may have been placed in suspension by the action of breaking waves in the surf zone or turbulence in rivers and streams or the agitation of waves outside of the breaker zone. Whatever the source, the material remains in suspension as the turbulence in the water column transports the material upwards, as it attempts to fall under the action of gravity.

In order to calculate the effect of the reduced wave height within the farm on the suspended sediments, it is first necessary to calculate the concentration of sediment over the depth. Since this is a function of the wave height (the wave height is a measure of the energy available to suspend the sediment), the concentration will be different inside and outside the farm. This concentration can in turn be integrated over the depth to determine the suspended load of the fluid. The difference will be the amount of material deposited in the farm region. (To determine time scales, further work is required to add the transporting ability of coastal currents, as they determine the rate at which the suspended load is brought into the farm.)

A model of the sediment concentration over the depth in the presence of waves can be described by

$$-\overline{C}w - \varepsilon \frac{\partial \overline{C}}{\partial z} = 0 \qquad (5.1)$$

where $\overline{C}$ is the mean concentration (averaged over a wave period)

w is the effective fall velocity

ε is an eddy viscosity

z is the vertical coordinate.

Recently, Hwang (1982) has solved this equation using an eddy viscosity which is proportional to the vertical orbital amplitude of the waves and found

$$C(z) = C_o \left(\frac{\tanh(kz/2)}{\tanh(kz_o/2)}\right)^{\frac{R\sinh kh}{\kappa Hk}} \left[1 - \frac{2\,W_o}{H\sigma} \frac{\sinh^2 kh(\coth kz - \coth kz_o)}{\kappa Hk}\right] \qquad (5.2)$$

where C_o is the concentration at elevation z_o

k is the wave number

R is a correction factor for the fall velocity reduction to the oscillatory wave field ($R \approx 0.07$)

κ is an eddy viscosity factor (0.4 assumed)

W_o is the mean fall velocity of the sediment

σ is the wave angular frequency ($2\pi/T$)

H is the wave height

and V is the variance of the bottom sediment distribution.

The reference concentration C_o is a function of the local bed shear stress and in general will be different inside the farm and out. Conservatively, C_o will be assumed to be the same in both locations and the differences in sediment load will be estimated using the following form:

$$\left(\frac{q}{C_o}\right) = \int_{-h}^{0} \left(\frac{C}{C_o}\right) dz \qquad (5.3)$$

Denoting the value of (q_1/C_o) as the suspended load outside the farm, the ratio of q/q_1 will denote the reduction of the ability of the water column to carry this load. This ratio is plotted in Figure 5.1 (as the lower bound of the shaded region). For most farm widths, a reduction of about 20% of the suspended load will occur (for this example). This means that this material will be deposited within the farm and within the first one or two wavelengths of the waves within the farm ($6 < kx < 12$).

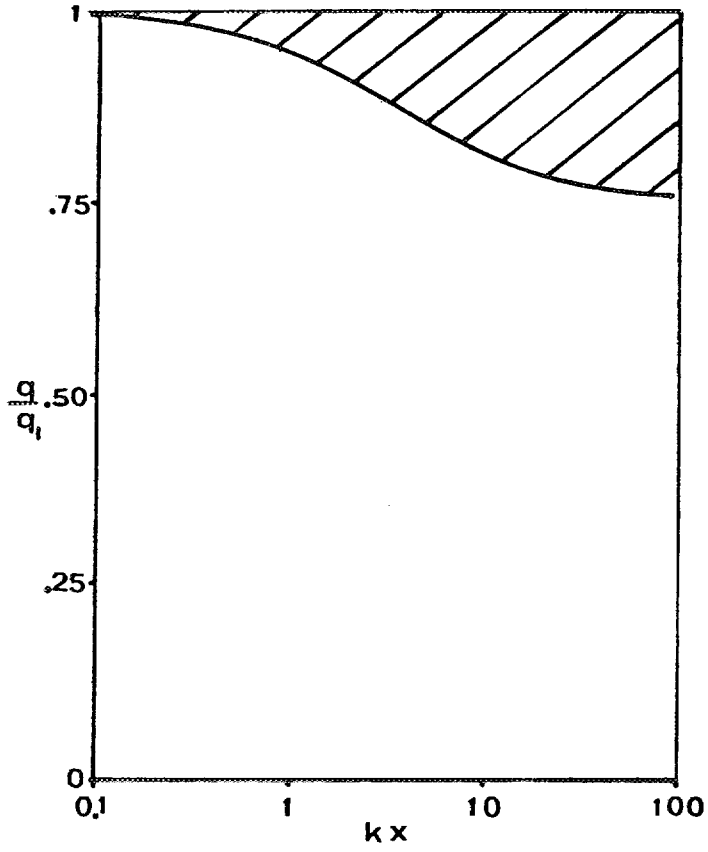

FIGURE 5.1 Reduction of Sediment Load With Dimensionless Distance Into Kelp Farm

Bottom scour will occur in and around the farm due to two major effects. The first is the deflection of the coastal currents around the farm as described by the parallel work at Argonne National Laboratory. Since sediment transport due to mean currents is proportional to some power of the velocity (say, 3-6), we can write

$$q_s \alpha V^m .$$

As the velocity increases slightly, the percentage increase in q_s is m times greater than the percentage increase in the velocity itself. Therefore, with knowledge of the increases of velocity due to the deflection of the farm, estimates of scour rates can be determined. Equilibrium bottom topography can be obtained from incipient motion criteria. In the vicinity of supports and anchors, scouring will also occur due to the same mechanism, but at a much smaller scale. The net result will be a settling of the anchors into the bottom (if it is sand) and subsequent burial.

VI. Conclusions and Recommendations

The presence of a dense array of kelp plants (artificially or naturally planted) reduces local wave heights, has an effect on the neighboring shoreline, experiences wave forces and changes the local sedimentation patterns. All of these effects have been examined in this study with the following conclusions:

(1) Wave heights can be significantly reduced as they propagate into the kelp farm. The amount of the reduction depends on the hydrodynamic and geometric characteristics of the waves and the kelp. A theoretical formulation has been developed for the convenient calculation of this damping.

(2) Locally, the wave field is disturbed due to the presence of the farm. Behind the farm is a shadow area which is a region of reduced wave heights. The size, particularly the shoreward extent of this shadow zone is important for coastal processes. A computer model of combined refraction/diffraction for water waves has been developed and tested. Graphical output shows the influence of various size farms on the local wave field.

(3) Wave forces on the kelp can be extreme under circumstances of combined waves and currents. Inertia forces should be included in any wave force calculation and first order analysis indicate these are of the same order of magnitude as the plant buoyancy.

(4) Local shoreline modifications are due to the shadow zone behind the farm. If the analog of an offshore breakwater is used, then shoreline modifications result which consist of the shoreline bulging out towards the farm. The amount of this bulge (called a tombolo) is dependent on the wave height reduction behind the farm and the amount of sediment transport along the adjacent shoreline. A tool to calculate this shoreline modification is the CERC model and an example was shown for the 20 ft design wave.

(5) Sedimentation will occur within the farm as the wave climate is reduced. A theoretical model for this has been discussed in Section V.

Data on local suspended sediments are necessary to complete this work. Local scour is expected around the anchors and at the outer edges of the farm due to the deflection of coastal currents. The magnitude depends on the strength of the natural current.

Further work is necessary to refine these analyses. This project has largely resulted in the development of models to illustrate the possible effects of the presence of a farm. These models must now be used with actual field data to enable an accurate depiction of future performance. Some of the measurements necessary or desirable are:

(1) Measurements of wave height attenuation through a natural stand of kelp.

(2) Remote sensing of wave refraction/diffraction due to a known kelp farm and also the resulting shoreline modifications

(3) Site specific wave climate data (height, period, direction and frequency of occurrence), current data, sediment data

(4) Wave force measurements on natural kelp.

Further analytical work needs to be done on the analytical predictions of wave forces on kelp (including the flexible nature of the plant) and on the perfection of the combined refraction/diffraction model (particularly for use over much larger areas).

VII. References

Bakker, W.T., "The Dynamics of a Coast With a Groyne System," Proc. of the 11th Conference on Coastal Engineering, ASCE, 1968, pp. 492-517.

Booij, N., Gravity Waves on Water With Non-Uniform Depth and Current, Ph.D. Diss., Tech. Univ. of Delft, Netherlands, 1981.

Berkhoff, J.C.W., "Computation of Combined Refraction/Diffraction," Proc. 13th International Coastal Engineering Conference, Vancouver, ASCE, 1972.

Dean, R.G., "Stream Function Representation of Nonlinear Ocean Waves," J. Geophys. Research, Vol. 20, No. 18, 1965.

Dean, R.G., "Equilibrium Beach Profiles: U.S. Atlantic and Gulf Coasts," Ocean Engineering Report No. 12, University of Delaware, 1977.

Dean, R.G. and Perlin, M., "Modelings of Sediment Transport from a Nearshore Dredge Disposal Area in the Vicinity of Oregon Inlet," COER Progress Report for CERC, Contract DACW 72-80-R-0030.

Dean, R.G. and Perlin, M., "A Numerical Model to Simulate Sediment Transport in the Vicinity of Coastal Structures," developed by the Coastal and Offshore Engineering and Research, Inc. for the Coastal Engineering Research Center, Technical Report-104, 1982(b).

Fulford, E., "Sediment Transport Distribution Across the Surf Zone," Masters Thesis, University of Delaware, 1982.

General Electric Company, Biomass Program Office, Advanced Energy Department, "System Functional Requirements and Specifications for a Nearshore Kelp to SNG Production Facility: Preliminary Engineering Study," King of Prussia, Pa., 1982.

Hwang, P.A., "Wave Kinematics and Sediment Suspension at Wave Breaking Point," Ph.D. Diss., Department of Civil Engineering, Univ. of Delaware, Newark, Delaware, 1982.

Ippen, A.T., ed., Estuary and Coastline Hydrodynamics, McGraw-Hill Book Company, New York, 1966.

Luke, J.C., "A Variational Principle for a Fluid With a Free Surface," J. Fluid Mech., Vol. 27, No. 2, 1967.

McGinn, J., "Deflection and Drag of Macrocystis Pyrifera in Uniform Currents," General Electric, PIR-U-1K8-81-91-664, King of Prussia, Pa., 1981.

Morison, J.R., O'Brien, M.P., Johnson, J.W. and Schaaf, S.A., "The Force Exerted by Surface Waves on Piles," Petrol. Trans., Vol. 89, 1950.

REFERENCES (CONTINUED)

Radder, A.C., "On the Parabolic Equation Method for Water Wave Propagation," J. Fluid Mech., 95, No. 1, 1979.

Savage, R.P., "Laboratory Study of the Effect of Groins on the Rate of Littoral Transport," BEB Technical Memorandum 114, 1959.

APPENDIX I Wave Height Reduction Due to Kelp

This Appendix presents an analysis of wave damping in the kelp field due to the drag force on the plants. The derivation is based on the conservation of energy equation. The assumptions are: linear wave theory is valid, plant motion can be neglected, the drag coefficient C_D is constant over the depth and the depth of water is a constant (i.e., a flat bottom).

Derivation

The conservation of energy equation is

$$\frac{\partial(EC_g)}{\partial x} = -\varepsilon_D \tag{I.1}$$

where E = wave energy/unit area = $1/2\ \rho g a^2$

ρ = fluid density

g = gravity

a = wave amplitude

C_g = wave group velocity = nC

$n = 1/2\ (1 + 2kh/\sinh 2kh)$

$C = \sqrt{(g/k)\tanh kh}$

k = wave number = $2\pi/L$

L = wave length

h = water depth

ε_D = energy dissipation

Considering the dissipation which is only due to the drag force, then

$$\varepsilon_D = F_D u \tag{I.2}$$

F_D = drag force on the plant

u = horizontal velocity due to the wave motion

Evaluating ε_D over the length of the plants,

$$\epsilon_D = \overline{\int_{-h}^{z} \frac{1}{2} \rho C_D A\, u|u| \cdot \; udz} \quad \cdot \; \# \text{ plant/unit area}$$

$$= Ba^3 \tag{I.3}$$

where $B = 2\rho \frac{C_D}{3\pi} \frac{D}{k} \frac{(\sinh^3 ks + 3 \sinh ks)}{3 \cosh^3 kh} \left(\frac{gk}{\sigma}\right)^3 \left(\frac{1}{b^2}\right)$

$s = h + z$ = elevation of the top of the plant relative to the bottom

b = spacing between plants.

Substituting Equation(I.3) into (I.1),

$$\frac{dEC_g}{dx} = \frac{1}{2} \rho g C_g \frac{da^2}{dx} = - Ba^3 \tag{I.4}$$

where C_g = constant due to constant depth assumption.

The solution of (I.4) is

$$\frac{a}{a_1} = \frac{1}{1 + B' \frac{a_1 x}{2}} \tag{I.5}$$

where $B' = B/(1/2\ \rho g\ C_g)$.

H_1 = incident wave height before entering the kelp field,

Writing in terms of wave height, and expressing the solution in dimensionless form,

$$\frac{H}{H_1} = \frac{1}{1 + \alpha kx} \tag{I.6}$$

where

$$\alpha = \frac{C_D}{3\pi} \left(\frac{D}{b}\right) \left(\frac{H_1}{b}\right) (\sinh^3 ks + 3 \sinh ks) \left(\frac{4}{3 \sinh kh\ (\sinh 2kh + 2kh)}\right) \tag{I.7}$$

Figure 2.1 in the text shows the function $H/H_1 = 1/(1 + \alpha\, kx)$. Table 2.1 in the text lists the values of parameter α under various wave and plant conditions.

Note from Equation (I.7), α is a function of 5 different parameters, C_D, D/b, ks, kH_1 and kh. The first three can be considered as plant-dependent, and the last two are wave-dependent.

To compute kh, Equation (2.4) must be solved. Rewriting Equation (2.4) it can be placed in the following form

$$F(kh) \equiv A - (kh)\tanh(kh) = 0$$

where $A = (\frac{2\pi}{T})^2 \frac{h}{g}$. The Newton-Raphson iterative technique finds a new kh, $(kh)_n$, based on an old estimate, $(kh)_o$, in the following fashion:

$$(kh)_n = (kh)_o - \frac{F((kh)_o)}{F'((kh)_o)}$$

where $F'((kh)_o) = -\tanh(kh)_o - (kh)_o \operatorname{sech}^2(kh)_o$. Only a few iterations are needed in general for an accurate solution. An initial value of kh might be 0.5.

APPENDIX II Parabolic Method for Combined Refraction/Diffraction of Water Waves

II.1 The Governing Equation

In 1967 Luke showed that the variational principle,

$$I = \int_{x_1}^{x_2} \int_{t_1}^{t_2} L \, dt \, dx \tag{II.1}$$

where

$$L = \rho \int_{-h}^{\eta} \left[\frac{(\hat{\phi}_x^2 + \hat{\phi}_y^2 + \hat{\phi}_z^2)}{2} + gz - \frac{\partial \hat{\phi}}{\partial t} \right] dz \tag{II.2}$$

correctly described the behavior of nonlinear water waves. Here $\hat{\phi}$ is the velocity potential of the wave motion, ρ is the fluid density and g is the acceleration of gravity. If we assume that $\hat{\phi}$ (x,y,z) can be represented as

$$\hat{\phi}(x,y,z) = \phi(x,y) \frac{\cosh k\,(h+z)}{\cosh kh} \tag{II.3}$$

where the cosh k(h+z) is the usual depth dependency associated with small amplitude wave theory, then after substitution into the Lagrangian L and performing the first variation yields a governing equation for the wave motion

$$\vec{\nabla} \cdot (nC^2 \vec{\nabla}\phi + n\sigma^2 \phi) = 0 \tag{II.4}$$

where $C = \sqrt{(g/k)\tanh kh}$, $n = \frac{1}{2}\left(1 + \frac{2kh}{\sinh 2kh}\right)$ and $\sigma = \frac{2\pi}{T}$.

T is the wave period. This model equation, which was developed by Berkhoff (1972) describes the shoaling, refraction and diffraction of waves. Booij (1981) shows that the inclusion of a term, $i\sigma f\phi$, in the equation results in wave damping and the parameter f is a measure of the damping.

Radder (1979) shows that with substitution $\bar{\phi} = \frac{\phi}{\sqrt{nC^2}}$ the equation can be placed in a standard hyperbolic form

$$\vec{\nabla}^2\bar{\phi} + k_c^2\,\bar{\phi} = 0 \tag{II.5}$$

where $$k_c^2 = k^2 + \frac{ifk}{nC} - \vec{\nabla}\left(\sqrt{nC^2}\right)/\sqrt{nC^2} \tag{II.6}$$

Assuming $\bar{\phi}$ is composed of a forward propagating component (ϕ^+) and a scattered (reflected) component, ϕ^-, the Helmholtz equation can be split, thus yielding an approximate equation for ϕ^+, the quantity of interest.

$$\frac{\partial^2\phi^+}{\partial y^2} + 2\,ik_c\,\frac{\partial\phi^+}{\partial x} + \left(2k_c^2 + i\,\frac{\partial k_c}{\partial x}\right)\phi^+ = 0 \tag{II.7}$$

One final substitution is made,

$$\phi^+ = e^{ik_o x}\,\psi(x,y), \tag{II.8}$$

which strips out the rapidly oscillating portion of the wave field. The k_o is a representative wave number.

The governing equation for ψ is then

$$\frac{\partial^2\psi}{\partial y^2} + 2ik_c\,\frac{\partial\psi}{\partial x} + F\psi = 0 \tag{II.9}$$

where $$F = k_c\left[2(k_c - k_o) + \frac{i}{k_c}\left(\frac{\partial k_c}{\partial x}\right)\right] \tag{II.10}$$

The numerical solution to this equation is obtained using a Crank-Nicholson integration procedure.

$$\frac{1}{2}\left(\frac{\psi_{i,j+1} - 2\psi_{i,j} + \psi_{i,j-1}}{(\Delta y)^2} + \frac{\psi_{i+1,j+1} - 2\psi_{i+1,j} + \psi_{i+1,j-1}}{(\Delta y)^2}\right) +$$

$$2i\, k_{c_{i,j}}\left(\frac{\psi_{i+1,j} - \psi_{i,j}}{\Delta x}\right) + F_{i,j}\left(\frac{\psi_{i+1,j} + \psi_{i,j}}{2}\right) = 0$$

where $F_{ij} = k_{c_{i,j}}\left[2(k_{c_{i,j}} - k_o) + \frac{1}{k_{c_{i,j}}}\frac{k_{c_{i+1,j}} - k_{c_{i,j}}}{\Delta x}\right]$ (II.11)

Or in matrix form

$$\begin{bmatrix} 1 & 0 & 0 & 0 & & 0 \\ \frac{1}{2(\Delta y)^2} & \frac{-1}{(\Delta y)^2} + \frac{i2k_{c_{i,2}}}{\Delta x} + \frac{F_{i,2}}{2} & \frac{1}{2(\Delta y)^2} & & & \\ & \frac{1}{2(\Delta y)^2} & \frac{-1}{(\Delta y)^2} + \frac{i2k_{c_{i,3}}}{\Delta x} + \frac{F_{i,3}}{2} & \frac{1}{2(\Delta y)^2} & & \\ & & \ddots & & & \\ & 0 & & & & \\ & & 0 & 0 & 1 & \end{bmatrix} \begin{bmatrix} \psi_{i,1} \\ \psi_{i,2} \\ \vdots \\ \psi_{i,JJ+1} \end{bmatrix}$$

$$= \begin{bmatrix} 1 \\ -\frac{1}{2(\Delta y)^2}\psi_{i-1,2} + \frac{F_{i-1,2}}{2}\psi_{i-1,2} - \frac{1}{2(\Delta y)^2}\psi_{i-1,2} \\ \vdots \\ 1 \end{bmatrix} \quad \text{(II.12)}$$

where the first and the last ($JJ+1^{th}$) equations are the boundary conditions and subject to change for different applications. The present set-up in Equation (II.11) is for the case of distant boundaries and no effect of the object is felt at the boundaries. Other boundary conditions will be discussed in a later section. The square matrix on the left hand side of Equation (II.11) is a tridiagonal matrix. Very efficient algorithms are readily available for its solution.

II.2 Boundary Conditions

As mentioned in the previous section, to enhance the computation of the parabolic formulation, the boundary values need to be specified. Equation (II.11) presented a formulation that the values at both boundaries are specified, which corresponds to the cases that the disturbance will not reach the boundaries and requires a tremendous area of computation. Other alternatives are (i) Reflective boundary conditions, (ii) Radiation conditions and (iii) Combination of radiation and fixed boundary conditions. Each will be discussed in detail below.

(i) Reflective boundary conditions

$$\frac{\partial \psi}{\partial y} = 0 \quad \text{at} \quad y = y_1 \quad \text{and } y = y_2 \tag{II.13}$$

where y_1 and y_2 are the left and the right hand side boundaries, or

$$\psi_1 = \psi_3 \; ; \; \psi_{JJ+1} = \psi_{JJ-1} \tag{II.14}$$

replacing the first and the last row of Equation (II.12).

Equation (II.13) uses central difference and is accurate to $O(\Delta y)^2$. This boundary condition is good for normal wave incidence and (1) solid boundaries or (2) periodic placement of the kelp farms. The disadvantage of this condition is that for oblique wave incidence, a shadow zone is created on the upstream side, and a standing wave zone on the downstream side of the computational area as shown in Figure II.1. The boundary effect will eventually propagate into the area of interest and introduce large errors.

(ii) Radiation boundary condition

$$\frac{\partial \psi}{\partial y} = ik_y \psi \quad \text{at } y = y_1 \text{ and } y = y_2 \tag{II.15}$$

based on the assumption that

$$\psi = |\psi| e^{-i(k_x x + k_y y)} e^{-i\sigma t} \tag{II.16}$$

where k_x and k_y are the wave numbers in the x- and y-direction, respectively. Combined with Equation (II.8) and write

$$\psi(x,y) = |\psi(x,y)| e^{i\beta} \tag{II.17}$$

therefore

$$\phi = \psi e^{ik_o x} e^{i\sigma t} = |\psi| e^{i(k_o x + \beta)} e^{-i\sigma t} \tag{II.18}$$

$$\text{since } \vec{k} = \vec{\nabla}(\vec{k}_o \cdot \vec{x} + \beta - \sigma t) \tag{II.19}$$

$$\text{so } k_y = \frac{\partial \beta}{\partial y} = \frac{\partial \tan^{-1}\left(\frac{\psi_{Im}}{\psi_{Re}}\right)}{\partial y} \tag{II.20}$$

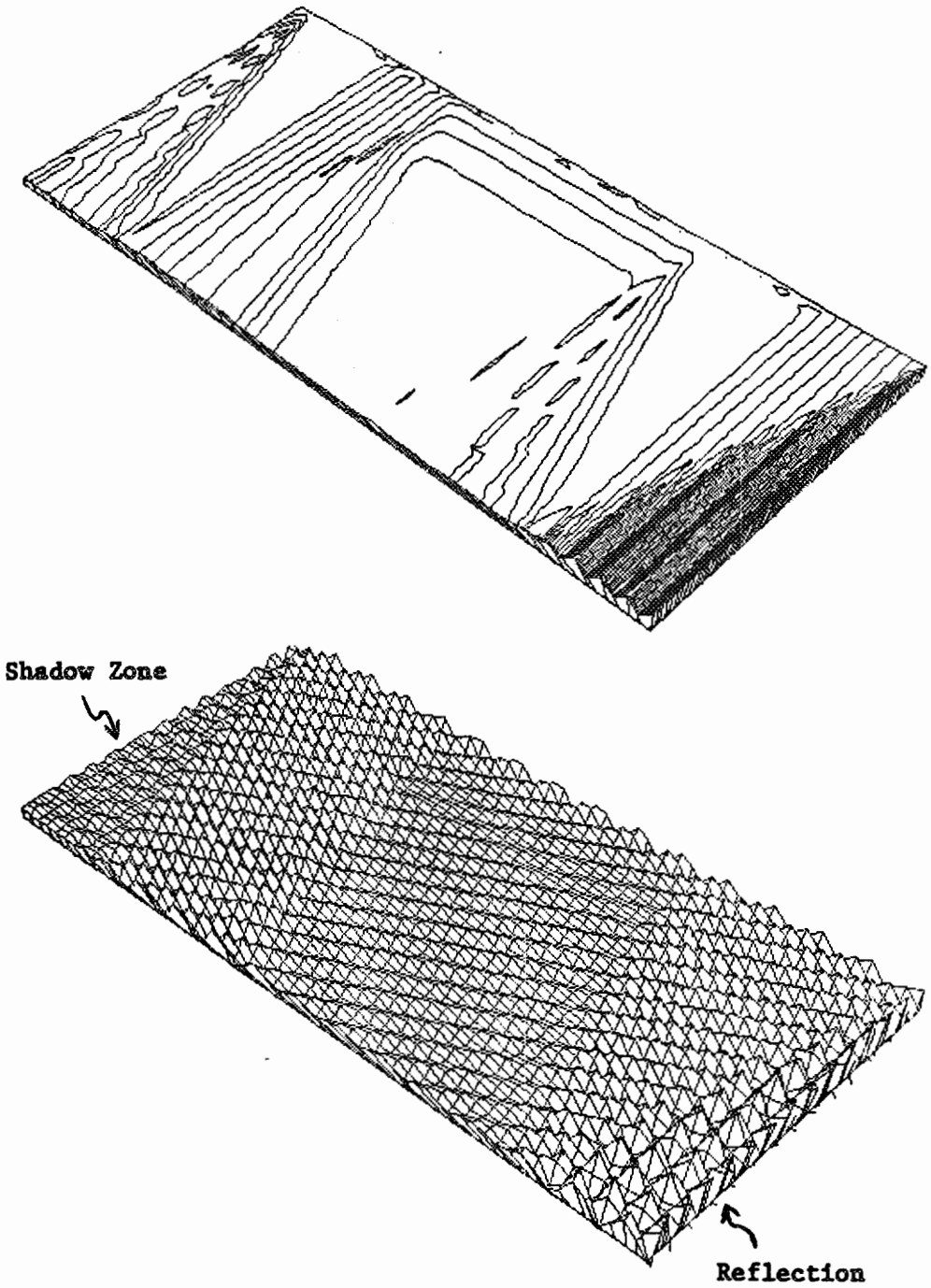

LEGEND:
NUMERICAL M= 60,N= 60,DX= 200.0,DY= 400.0,B.C. CODE= 0
WAVE: T= 20.0,DPT REF= 50.00,L REF= 781.95,H REF= 20.00,THETA= 30.00
BOTTOM CODE: 0,SLOPE OR A VALUE= 0.00000
KELP: ELV/DPT=1.0,DIA=1.0,SPACING= 10.00,FARM LENGTH-Y (GRID)= 24,WIDTH= 15
F DAMP= 1.0000
PLOTTED FROM (UPPER LEFT CORNER): 1 1 PLOTTED SIZE (X BY Y): 60 60
#?
#ET=12:19.8 PT=19.3 IO=31.9

FIGURE II.1 Reflective Boundary Conditions

Equation (II.15) becomes

$$\frac{\psi_{i+1,j+1} - \psi_{i+1,j-1}}{2\Delta y} = ik_{y_{i+1,j}} \psi_{i+1,j} \tag{II.21}$$

In practice, k_y is evaluated using $\psi_{i,j+1}$ and $\psi_{i,j-1}$. Figure II.2 shows a plot based on the above formulation. For normal incidence, this scheme is equivalent to reflective boundary conditions. For oblique incidence, the downstream boundary is well taken care of. The upstream side, however, created certain anomaly for some unknown reason. A third boundary condition that fix the upstream condition is, therefore, considered.

(iii) Fixed-value upstream and radiation downstream conditions.

To remedy the upstream boundary condition, the waves on this boundary are assumed fixed, i.e.,

$$\phi = e^{i(k_x x + k_y y_1)} \tag{II.22}$$

or equivalently

$$\psi = (e^{ik_x x + ik_y y_1})/e^{ik_o x} \tag{II.23}$$

where
$$\begin{aligned} k_x &= k_c \cos\theta \\ k_y &= k_c \sin\theta \end{aligned} \tag{II.24}$$

and θ is wave incidence angle.

The downstream side is still treated with radiation condition, Equation (II.21). The result was shown in Figure 2.5 in the text. The result is satisfactory and only introduced less than 4% error on both boundaries in the range of computation. However, since this scheme reflects the scattered wave, it will introduce errors for very far field computation.

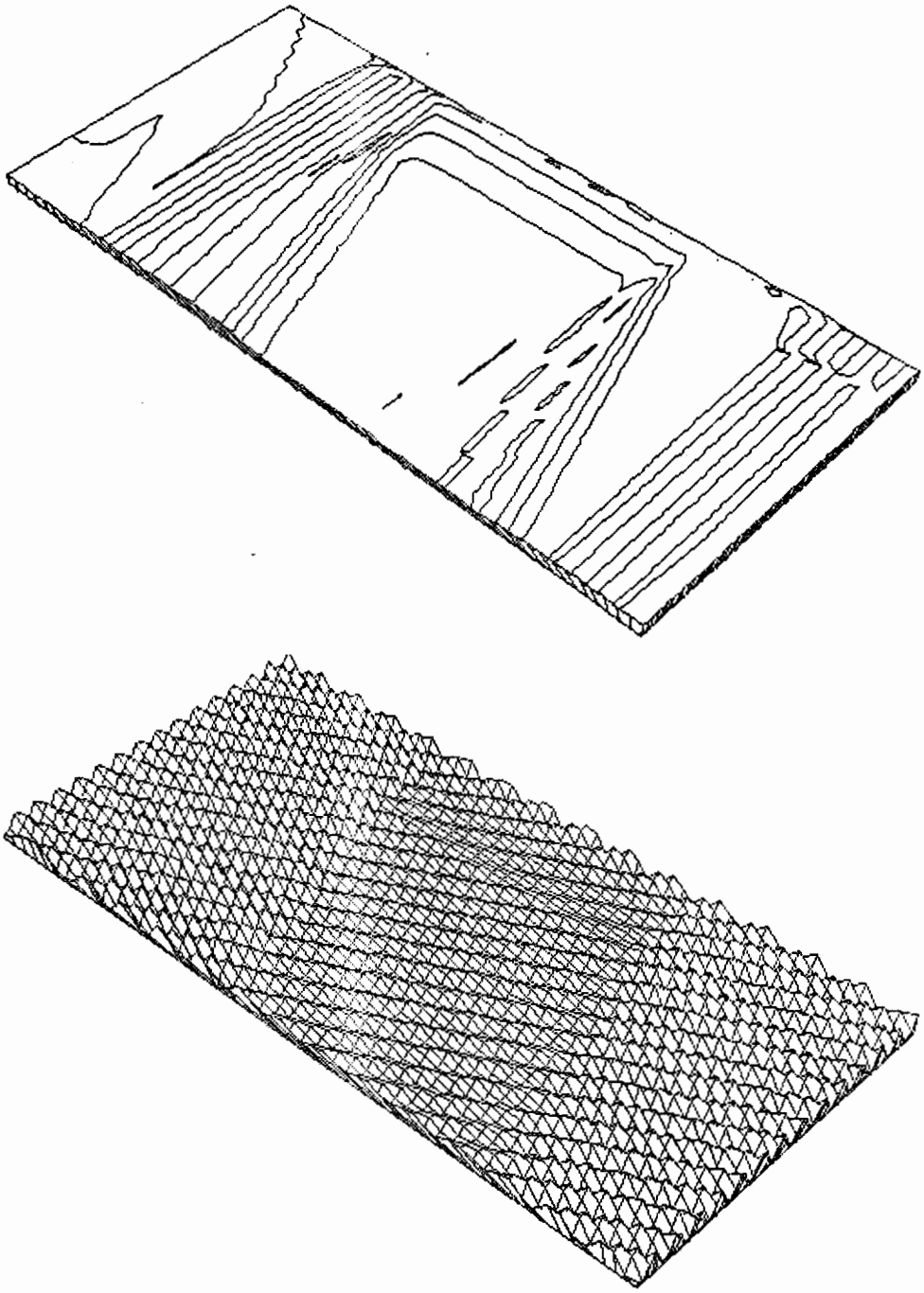

LEGEND:
NUMERICAL M= 60,N= 60,DX= 200.0,DY= 400.0,B.C. CODE= 1
WAVE: T= 20.0,DPT REF= 50.00,L REF= 781.95,H REF= 20.00,THETA= 30.00
BOTTOM CODE: 0,SLOPE OR A VALUE= 0.00000
KELP: ELV/DPT=1.0,DIA=1.0,SPACING= 10.00,FARM LENGTH-Y (GRID)= 24,WIDTH= 15
F DAMP= 1.0000
PLOTTED FROM (UPPER LEFT CORNER): 1 1 PLOTTED SIZE (X BY Y): 60 60
#?
#ET=10:20.3 PT=19.6 IO=32.0

FIGURE II.2 Radiation Conditions for Both Lateral Boundaries

Although, all the schemes discussed are good for short range computation, Scheme (iii) is obviously much superior than the others and is chosen for the design computation.

II.3 Testing of the Numerical Scheme

Various tests of the numerical scheme were conducted to examine the optimum grid sizes and verify the accuracy of the model. These tests follow.

(i) The optimal grid size for computation

Figures II.3, II.4 and II.5 are computations using 6, 4 and 3 grids per wave length, respectively. The kelp farm size was kept constant (3120' x 1820'). The contours of the wave height (K_I) were similar (note that all plots are 60 grids x 60 grids, therefore, representing different computation sizes), but the resolution for individual wave decreases with increasing grid size. For the case of three grids/wave length, ambiguity in the direction of wave propagation is obvious. It is decided that four grids/wave length is the optimal size to use.

Figure II.6 presents the computation using unequal grid-size, $\Delta y = 2\Delta x$, and $L/\Delta x \approx 4$. This rectangular grid is recommended for large kelp farm computations.

(ii) Accuracy in wave representation

Figure II.7 presents a case where the waves enter a region of constant depth with a 30° angle. The wave height error is $\pm$ 4% all over and is not presented. It is clear that the wave information is correctly represented under the present numerical scheme. For mild scattering, the error remains in that order as discussed in the last section.

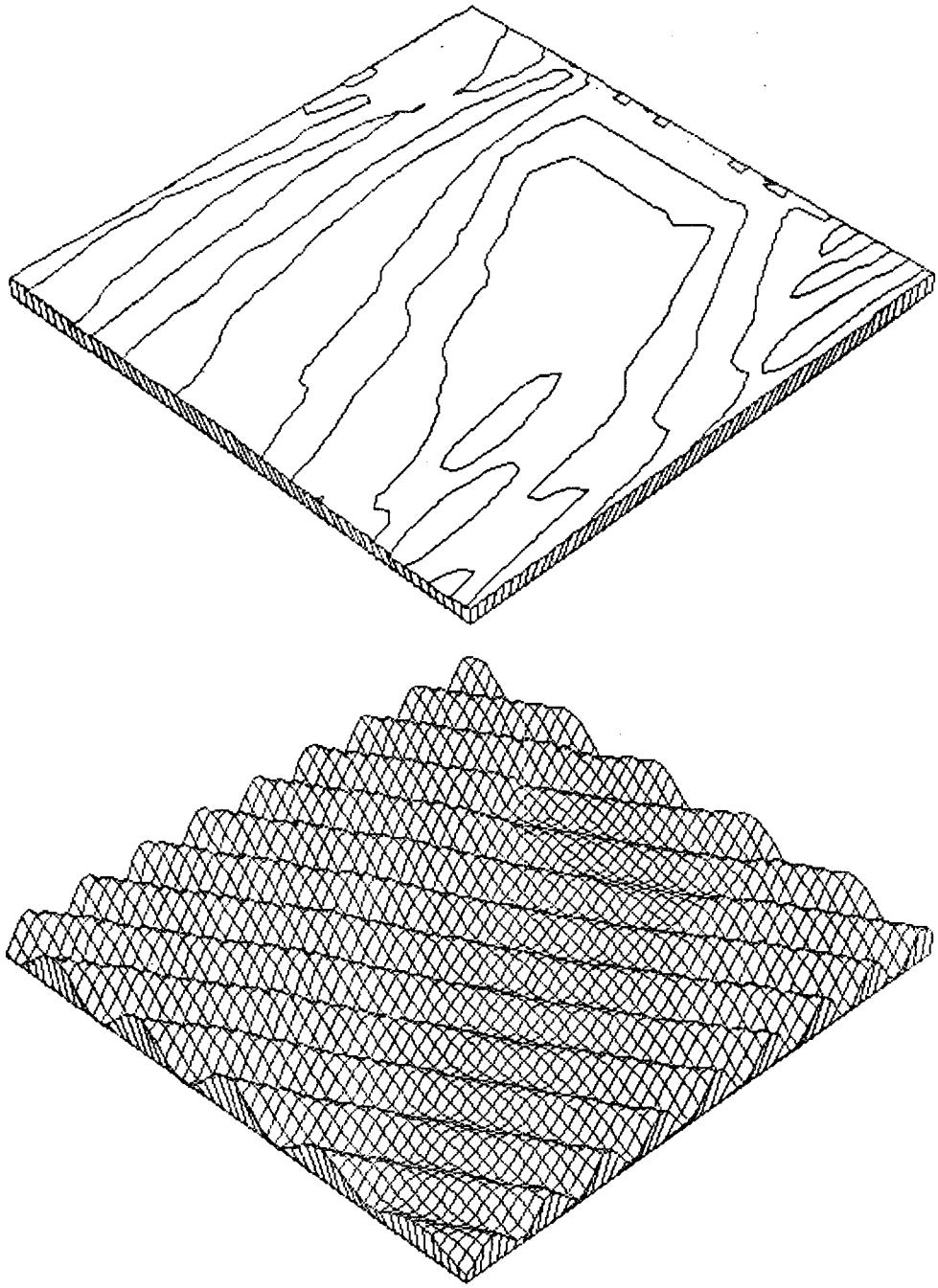

LEGEND:
NUMERICAL M= 60,N= 60,DX= 130.0,DY= 130.0,B.C. CODE= 2
WAVE: T= 20.0,DPT REF= 50.00,L REF= 781.95,H REF= 20.00,THETA= 30.00
BOTTOM CODE: 0,SLOPE OR A VALUE= 0.00000
KELP: ELV/DPT=1.0,DIA=1.0,SPACING= 10.00,FARM LENGTH-Y (GRID)= 24,WIDTH= 14
F DAMP= 1.0000
PLOTTED FROM (UPPER LEFT CORNER): 1 1 PLOTTED SIZE (X BY Y): 60 60
#?
#ET=8:17.5 PT=18.2 IO=32.4

FIGURE II.3 Wave Field With 6 Grid Points Per Wave

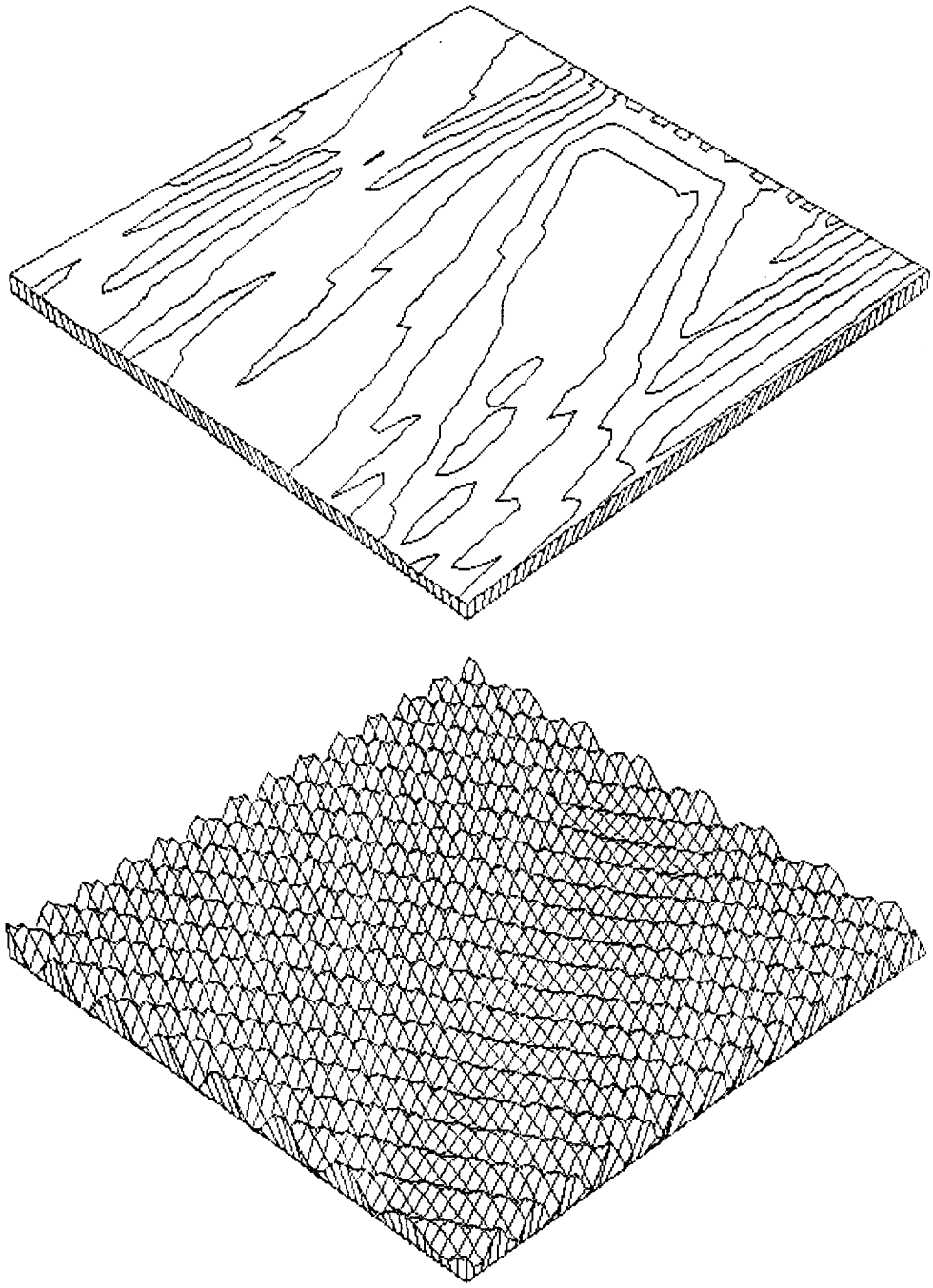

LEGEND:
NUMERICAL M= 60,N= 60,DX= 200.0,DY= 200.0,B.C. CODE= 2
WAVE: T= 20.0,DPT REF= 50.00,L REF= 781.95,H REF= 20.00,THETA= 30.00
BOTTOM CODE: 0,SLOPE OR A VALUE= 0.00000
KELP: ELV/DPT=1.0,DIA=1.0,SPACING= 10.00,FARM LENGTH-Y (GRID)= 16,WIDTH= 9
F DAMP= 1.0000
PLOTTED FROM (UPPER LEFT CORNER): 1 1 PLOTTED SIZE (X BY Y): 60 60
#?
#ET=8:14.0 PT=17.0 IO=35.2

FIGURE II.4 Wave Field With 4 Grid Points Per Wave

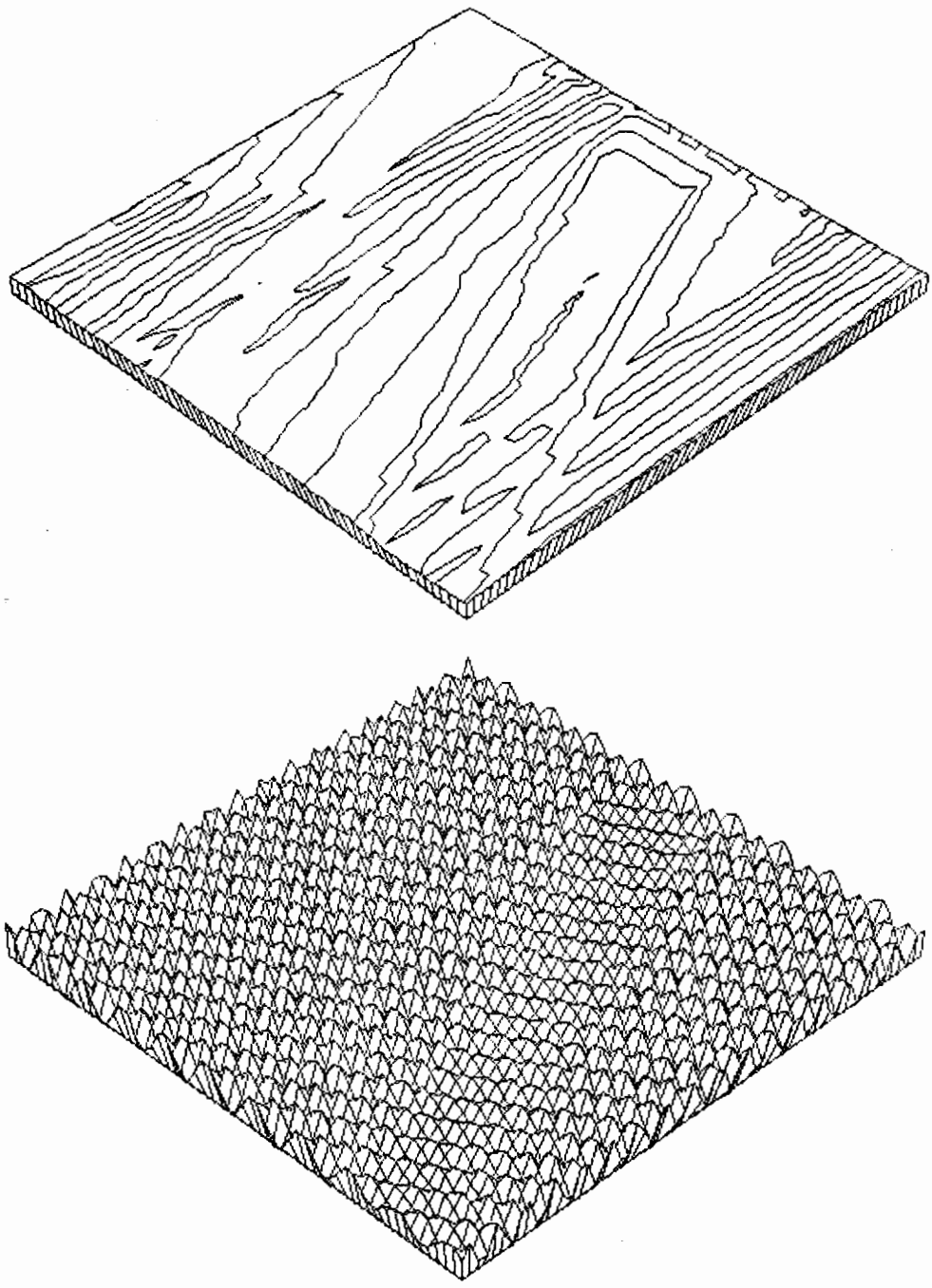

LEGEND:
NUMERICAL M= 60,N= 60,DX= 260.0,DY= 260.0,B.C. CODE= 2
WAVE: T= 20.0,DPT REF= 50.00,L REF= 781.95,H REF= 20.00,THETA= 30.00
BOTTOM CODE: 0,SLOPE OR A VALUE= 0.00000
KELP: ELV/DPT=1.0,DIA=1.0,SPACING= 10.00,FARM LENGTH-Y (GRID)= 12,WIDTH= 7
F DAMP= 1.0000
PLOTTED FROM (UPPER LEFT CORNER): 1 1 PLOTTED SIZE (X BY Y): 60 60
#?
#ET=9:19.8 PT=19.2 IO=32.1

FIGURE II.5 Wave Field With 3 Grid Points Per Wave

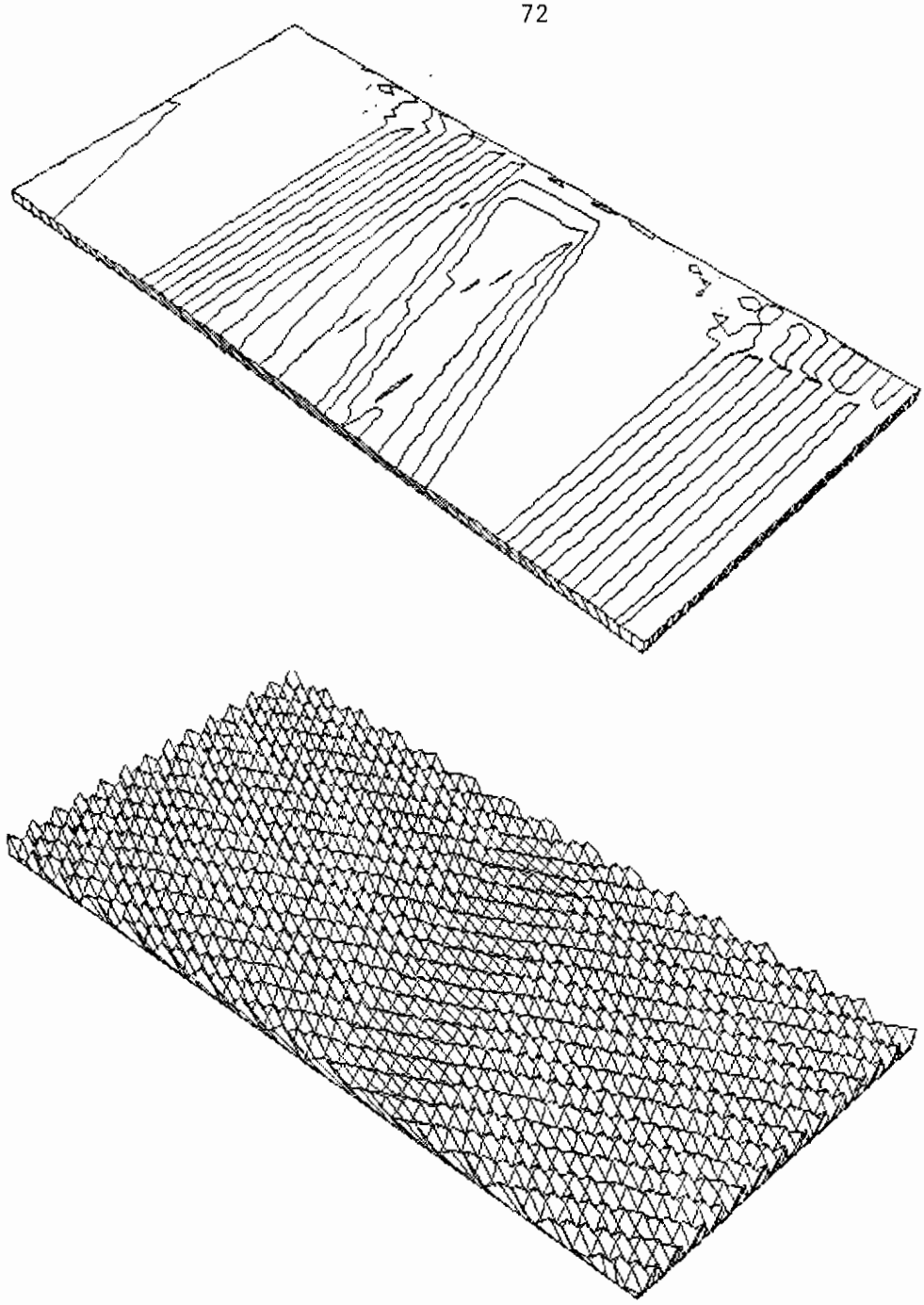

```
LEGEND:
NUMERICAL M=  60,N=  60,DX= 200.0,DY= 400.0,B.C. CODE= 2
WAVE: T= 20.0,DPT REF= 50.00,L REF= 781.95,H REF= 20.00,THETA= 30.00
BOTTOM CODE: 0,SLOPE OR A VALUE= 0.00000
KELP: ELV/DPT=1.0,DIA=1.0,SPACING=  10.00,FARM LENGTH-Y (GRID)=  8,WIDTH=  9
 F DAMP=  1.0000
PLOTTED FROM (UPPER LEFT CORNER):   1   1 PLOTTED SIZE (X BY Y):  60  60
#?
#ET=8:42.0 PT=18.2 IO=36.1
```

FIGURE II.6 Wave Field With $\Delta y = 2\Delta x$

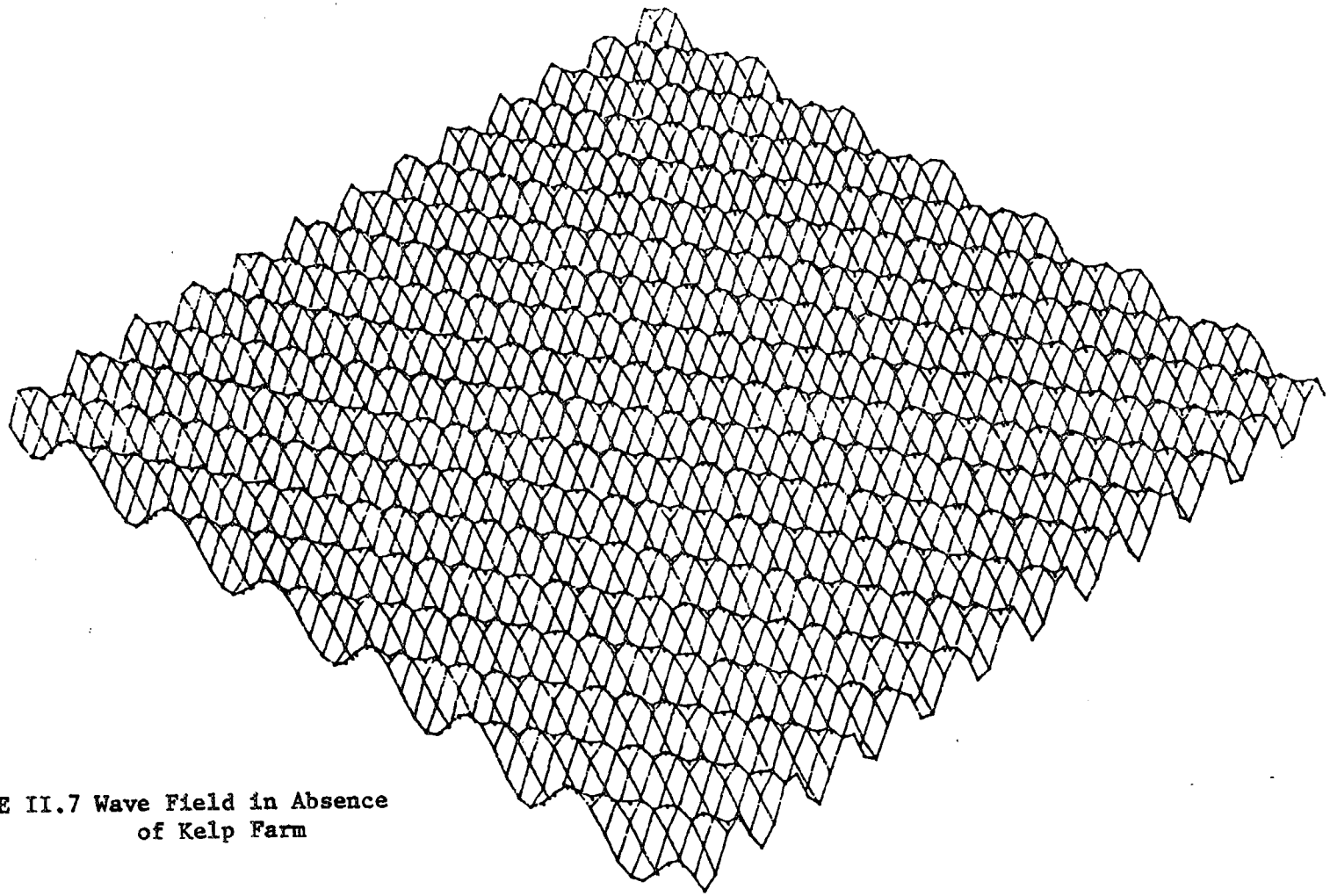

FIGURE II.7 Wave Field in Absence of Kelp Farm

```
INPUT S1,S2,S3 (50,100,5000) AND S4,S5,S6 (10,20,0)
#?
200,200,200,30,30,0
JOB? (1=AMP, 2=INSTAN WAVE)
2
IDEV, AMP FAC OF DATA
30,2
N=60, M=60, DY=200.0, DX=200.0, T=20.0, DPTREF=60.0, THETA=0.523598775866, RKO=0
.0073739763115, FWKELP=0.0, KWIDE=4, KLENG=4,
```

(iii) Calibration with the analytical result of wave diffraction from a solid breakwater (Shore Protection Manual, 1977)

Figures II.8a and II.9a simulate wave diffraction pattern beyond an offshore breakwater. The corresponding analytical solutions are presented in Figures II.8b and II.9b. The present numerical computation predicted somewhat large wave height, max 1.26 along the ridge, while the theoretical result gives 1.14. The general patterns are similar.

Based on this and the previous paragraph, the final choice of the numerical parameters are: $\Delta x \simeq 1/4$ L, $\Delta y = 2\Delta x$ and combination of fixed upstream and radiation downstream boundary conditions.

II.4 Relation of f to the Physical Parameters

The damping coefficient f in Equation (II.6) is related to the kelp and wave parameters such as drag coefficient, effective kelp diameter, effective kelp spacing, kelp height, wave height, wave period and water depth by comparing the one-dimensional solution of Equation (II.5) to the solution obtained in Appendix I, (I.6).

The one dimensional solution of Equation (II.5) is

$$\phi = A\, e^{ik_c x - \sigma t} \tag{II.25}$$

denote $k_c = k_r + ik_i$ (II.26)

where k_r, k_i are real and positive, then the decay of wave height can be expressed as

$$\frac{H}{H_1} = e^{-k_i x} \tag{II.27}$$

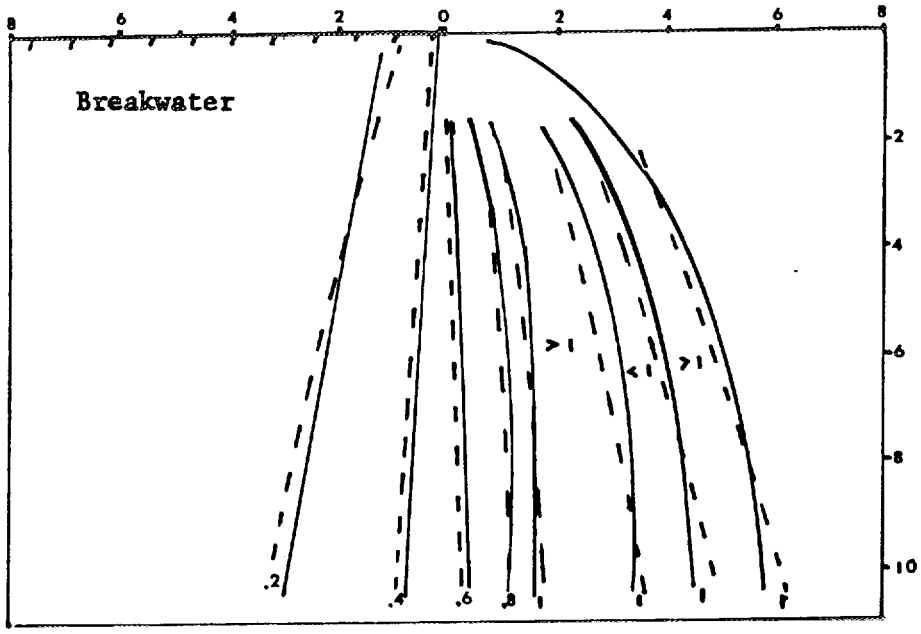

——— Theoretical (Penny and Price, 1952)
----- Parabolic Model

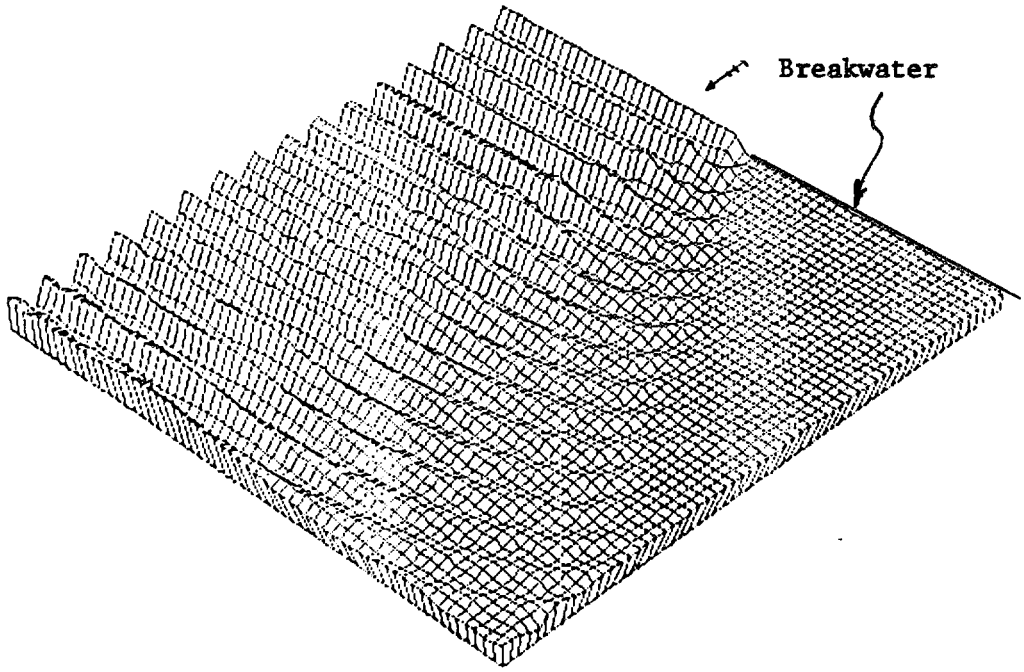

FIGURE II.8 Diffraction Behind Breakwater: Normal Incidence

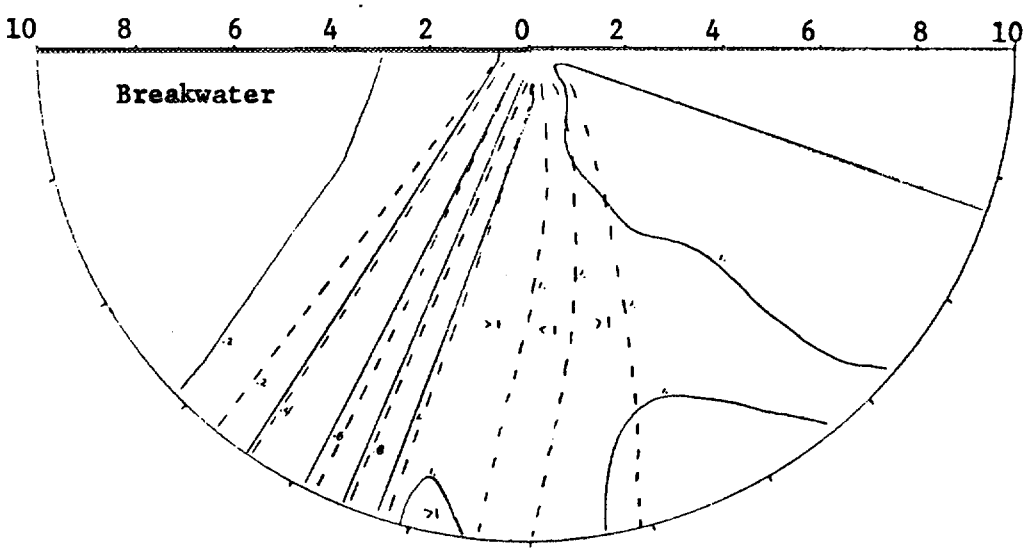

——— Theoretical (Shore Protection Manual, 1977)
------ Parabolic Model

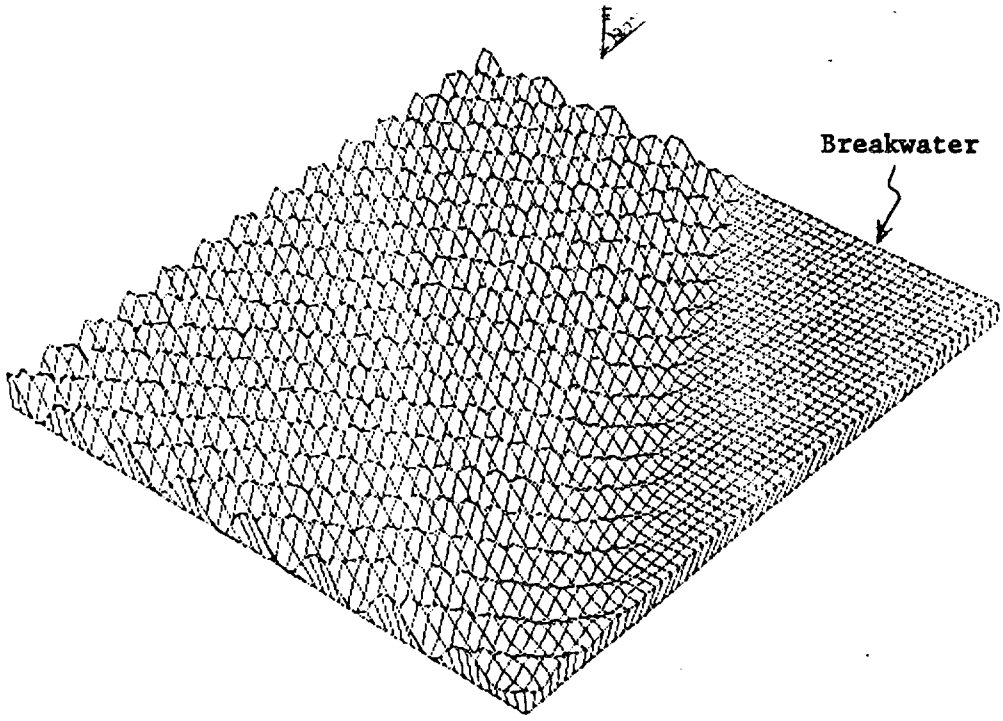

FIGURE II.9 Diffraction Behind Breakwater: 30° Incidence

The relationship of f to the kelp parameters can be derived from Equations (II.26), (II.6) and (I.6) as follows. Equating (II.26) to (II.6), we found

$$\left.\begin{aligned} &\left(\frac{k_r}{k}\right)^2 \qquad \left(\frac{h_i}{k}\right)^2 = 1 \\ &2\,\frac{k_r}{k}\,\frac{k_i}{k} = \frac{f}{n\sigma} \end{aligned}\right\} \tag{II.28}$$

where k is the wave number for no-damping condition. The solution of Equation (II.28) is

$$k_i = k\sqrt{\frac{-1+\sqrt{1+\left(\frac{f}{n\sigma}\right)^2}}{2}} \tag{II.29}$$

and

$$k_r = k\sqrt{\frac{1+\sqrt{1+\left(\frac{f}{n\sigma}\right)^2}}{2}} \tag{II.30}$$

On the other hand, equating (II.27) to (I.6), we found that

$$k_i x = \ell n(1+\alpha k x) \tag{II.31}$$

Substituting Equation (II.29) into (II.31), then

$$f = n\sigma\ \{[2(\frac{\ell n(1+\alpha b x)}{kx})^2 + 1]^2 - 1\}^{1/2} \tag{II.32}$$

where α is expressed in Equation (I.7) and rewritten here for convenience,

$$\alpha = \frac{C_D}{3\pi}\left[\frac{D}{b}\right]\left[\frac{H_1}{b}\right][\sinh^3 ks + 3\sinh ks]\left[\frac{4}{3\sinh kh(\sinh^2 kh+2kh)}\right] \tag{I.7}$$

For small values of αkx, the natural logarithm of $(1+\alpha kx)$ can be replaced by a power series expansion which yields (using only the first term):

$$f = n\sigma \{(2\alpha^2+1)^2-1\}^{1/2} \qquad \text{(II.33)}$$

For further approximating,

$$f = n\sigma\, 2\alpha \qquad \text{(II.34)}$$

Here f is not a function of position and is conveniently expressed linearly with α. For the computer model, however, Equation (II.32) is used.

APPENDIX III. Modeling of Sediment Transport in the Nearshore

Introduction

A summary of the numerical model for shoreline modification developed by COER (Dean and Perlin, 1982) is given in this Appendix.

Computational Scheme

The model is an n-line representation of the surf zone in which the longshore direction is divided into equal segments each Δx in length. The bathymetry is represented by n-contour lines, each of a specified depth, which change in location according to the equation of sediment conservation. There are two components of sediment transport at each of the contour lines - a longshore component and an offshore component. Figure III.1 is a definition sketch showing the beach profile represented by a series of steps, the planform profile representation and the notation used.

Distribution of Longshore Sediment Transport Across the Nearshore Zone

Based on model tests by Savage (1959) as interpreted by Fulford (1982), COER has developed a distribution of longshore sediment transport across the surf zone as

$$Q_x(y) = C' H_b^{5/2} \, e^{-\frac{h^{3/2} + H_b A^{3/2}}{1.25\, h_b}} \sin 2\,(\theta - \alpha_c) \qquad \text{(III.1)}$$

in which C' represents the coefficiant in the usual longshore sediment transport equation, θ is the averaged wave angle at the location, α_c is the local contour orientation angle, h_b and H_b are the breaking water depth and wave height and A is the scale parameter associated with the equilibrium beach

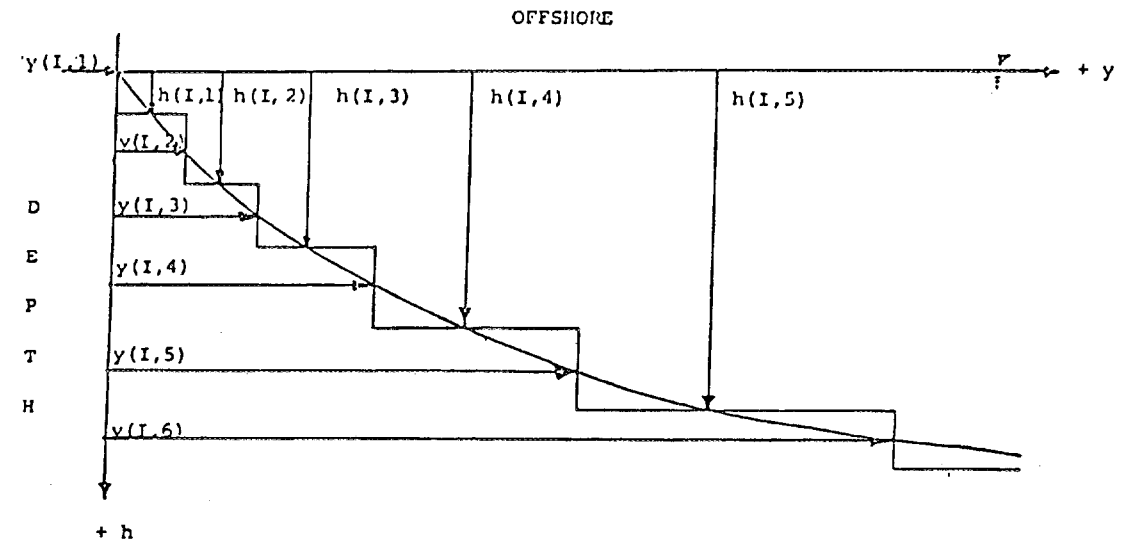

a) Beach Profile Representation

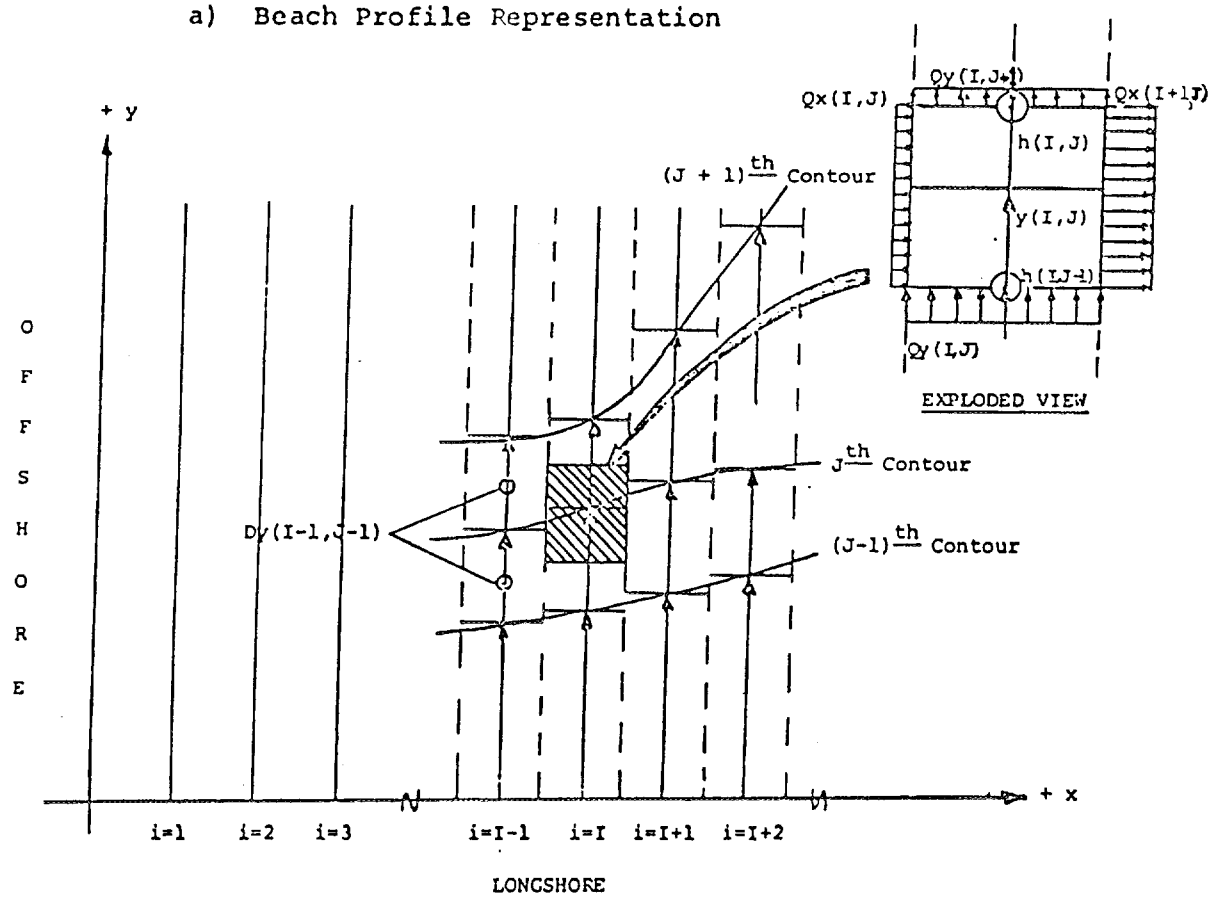

b) Beach Planform Representation

FIGURE III.1 Definition Sketch.

profile (to be described in more detail later).

Onshore-Offshore Sediment Transport

The equation governing onshore-offshore transport Q_y is based on the approach introduced by Bakker (1968),

$$Q_{yi,j} = K(h) \left[y_{i,j-1} - y_{i,j} + w_{i,j}\right] \tag{III.2}$$

in which w is the equilibrium spacing associated with the contour locations. Thus if the slope is greater than equilibrium, offshore transport results and vice versa. The parameter K(h) is an "activity factor" which based on our earlier work, primarily within the surf zone, was found to be

$$K = 10^{-5} \text{ ft/sec} \quad , \quad h < h_b$$

To generalize this concept for transport seaward of the surf zone, the wave energy dissipation per unit volume was utilized as a measure of mobilization of the bottom sediment. Inside the surf zone, the dominant wave energy dissipation is caused by wave breaking, whereas outside the surf zone, the dominant mode of wave energy dissipation is due to bottom friction. These two components will be denoted by D_1 and D_2, respectively.

Energy Dissipation by Wave Breaking - The wave energy dissipation per unit volume by wave breaking, D_1, is

$$D_1 = \frac{1}{h} \frac{\partial}{\partial y} (E\ C_G) \tag{III.3}$$

which, employing the spilling breaker assumption ($H = \kappa h$) within the surf zone, can be shown to be

$$D_1 = \frac{5}{16} \rho g^{3/2} \kappa^2 h^{1/2} \frac{\partial h}{\partial y} \tag{III.4}$$

or

$$D_1 = \frac{5}{24} \rho g^{3/2} \kappa^2 A^{3/2} \tag{III.5}$$

in which A is a scale parameter in the equilibrium beach profile (Dean, 1977)

$$h(y) = Ay^{2/3} \tag{III.6}$$

Energy Dissipation by Bottom Friction - The wave energy dissipation per unit volume due to bottom friction, D_2, is

$$D_2 = \frac{1}{h} \tau u_b = \frac{1}{h} \rho C_f \overline{|u_b| u_b^2} \tag{III.7}$$

in which C_f is a bottom friction coefficient, u_b is the bottom water particle velocity and the overbar indicates a time average. For linear waves, Equation (III.7) can be reduced to

$$D_2 = \frac{1}{6\pi} \frac{\rho}{h} C_f \frac{H^3 \sigma^3}{\sinh^3 kh} \tag{III.8}$$

The activity coefficient, K, outside of the surf zone, is expressed as

$$K = \frac{1}{\Gamma} \frac{D_2}{D_1} \times 10^{-5} \text{ ft/sec} \quad , \quad h > h_b \tag{III.9}$$

$$K = \frac{4}{5\Gamma} \frac{C_f \sigma^3}{g^{3/2} \kappa^2 A^{3/2} h} \left(\frac{H}{\sinh kh}\right)^3 \times 10^{-5} \tag{III.10}$$

in which Γ is a parameter relating the efficiency with which breaking wave energy (which occurs primarily near the water surface) mobilizes the sediment bottom ($0 < \Gamma < 1$).

Figure III.2 presents an example of the variation of the activity coefficient versus relative depth for a particular wave period and deep water wave height. It is seen that the activity coefficient K reduces rapidly with increasing depth.

Equation of Continuity

The equation of continuity, finite differenced for the n^{th} and $(n+1)^{th}$ time-steps can be written as

$$\frac{y_{i,j}^{n+1}-y_{i,j}^{n}}{\Delta t} = \frac{1}{2\Delta x\Delta h}\{Q_{xi,j}^{n+1}+Q_{xi,j}^{n}-Q_{xi+1,j}^{n+1}-Q_{xi+1,j}^{n}+Q_{yi,j}^{n+1}+Q_{yi,j}^{n}-Q_{yi,j+1}^{n+1}-Q_{yi,j+1}^{n}\} \quad \text{(III.11)}$$

Defining $R_{i,j}$ as $\frac{1}{2\Delta x\Delta h}$, inserting Equations (III.1) and (III.2) into Equation (III.11), and transferring all known quantities for the n^{th} time-step to the right-hand side of the equation results in

$$y_{i,j}^{n+1}+(\Delta tR_{i,j})S3_{i,j}y_{i,j}^{n+1}-(\Delta tR_{i,j})S3_{i,j}y_{i-1,j}^{n+1}-(\Delta tR_{i,j})S3_{i+1,j}y_{i+1,j}^{n+1}$$

$$+(\Delta tR_{i,j})S3_{i+1,j}y_{i,j}^{n+1}-(\Delta tR_{i,j}\text{Const }6_{i,j})[\tfrac{1}{2}(y_{i,j-1}^{n+1}-y_{i,j}^{n+1})]$$

$$+(\Delta tR_{i,j}\text{Const }6_{i,j+1})[\tfrac{1}{2}(y_{i,j}^{n+1}-y_{i,j+1}^{n+1})] = (AWARE)_{i,j} \quad \text{(III.12)}$$

Equation (III.12) can be rewritten as

$$(1+U+V+Z1+Z2)y_{i,j}^{n+1}-(U)y_{i-1,j}^{n+1}-(V)y_{i+1,j}^{n+1}$$

$$-(Z1)y_{i,j-1}^{n+1}-(Z2)y_{i,j+1}^{n+1} = (AWARE)_{i,j} \quad \text{(III.13)}$$

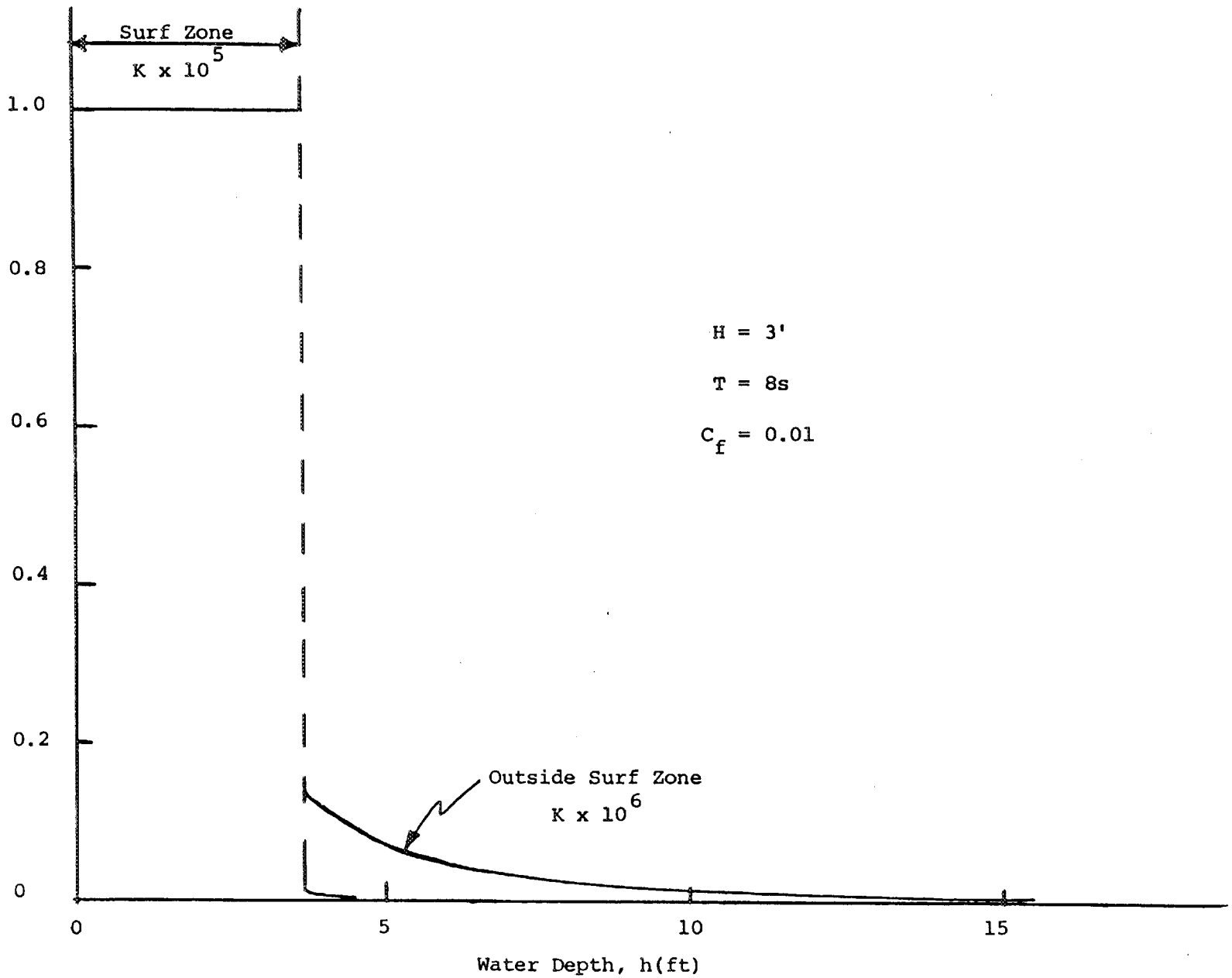

FIGURE III.2 Example of Activity Coefficient, K, vs. Water Depth, h, For Particular Wave Conditions.

where $U = \Delta t R_{i,j} S3_{i,j}$

$V = \Delta t R_{i,j} S3_{i+1,j}$

$Z1 = (\frac{\Delta t}{2}) R_{i,j} \text{Const } 6_{i,j}$

$Z2 = (\frac{\Delta t}{2}) R_{i,j} \text{Const } 6_{i,j+1}$

Equation (III.13) is a weighted, centered scheme in which $y_{i,j}^{n+1}$ is computed using a weighting of itself and its four adjacent "neighbors." The weighting factors (U,V,Z1 and Z2) are functions of the wave climate, the slope between contours and the other variables included in the original formulation. Investigation of a small, gridded system demonstrates that by writing simultaneous equations, one for each $y_{i,j}^{n+1}$, a banded matrix results. It can be solved using one of the available routines from the International Math and Statistics Library (IMSL), LEQT1B. A schematic representation of the matrix A which results from the matrix equation Ay = B is presented in Figure III.3. In this schematic, the large zeros represent triangular corner sections of all zeros, the 0...0 represent bands of zeros, the number of which are dependent on the number of contours simulated [the number of zero bands between either remote non-zero bands, and the tridiagonal non-zero bands equals two less than the number of contours modeled (in both the upper and lower co-diagonals of the matrix)].

Of course, the matrix requires boundary values on both longshore extremities and both on and offshore boundaries. The longshore boundary conditions are handled by modeling a sufficient stretch of shoreline so that the effects of any structure or other perturbation are minimal. The y-values along these boundaries can, therefore, be fixed at their initial locations. In the on-offshore direction, boundaries are handled quite differently. The

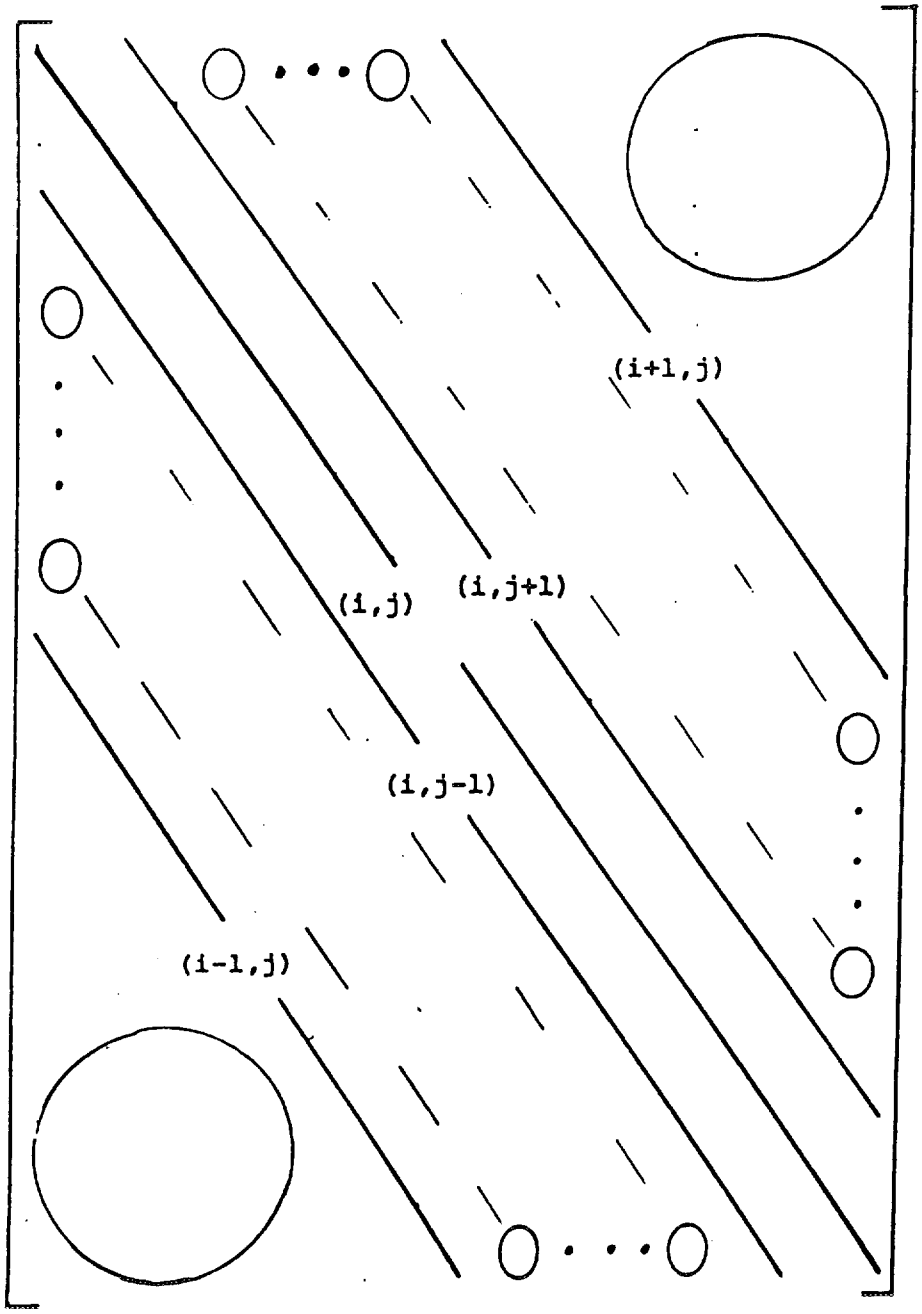

NOTE: SIZE OF MATRIX-FULL STORAGE MODE
[(IMAX-2)(JMAX) x (IMAX-2)(JMAX)]

SIZE OF MATRIX-BANDED STORAGE MODE
[(IMAX-2)(JMAX) x (2JMAX + 1)]

FIGURE III.3 Schematic Representation of Banded Matrix If Not Stored in Banded Storage Mode.

berm and beach face are assumed to move in conjunction with the shoreline position. The required sediment transport is then computed by the change in position of the shoreline. The two equations are

$$y_{i,0}^{n+1} = y_{i,0}^{n} + (y_{i,1}^{n+1} - y_{i,1}^{n}) \tag{III.14}$$

$$Q_{yi,1}^{n+1} = -(\frac{\text{Berm } \Delta x}{\Delta t})(y_{i,1}^{n+1} - y_{i,1}^{n}) \tag{III.15}$$

The offshore boundary is handled by keeping $y_{i,jmax+1}^{n+1}$ (the contour beyond the last simulated contour) fixed, unless the angle of repose is exceeded. Then, the $y_{i,j\ max+1}^{n+1}$ is reset (at the conclusion of the n+1 time-step) to a position such that the slope equals the angle of repose. Note that $y_{i,0}^{n+1}$ is represented in the program by $\hat{y}zero_i$.